2017

SECOND-LIFE BATTERY ELECTROCHEMICAL IMPEDANCE SPECTROSCOPY MODELING AND APPLICATION TO A RESIDENTIAL SYSTEM

Busra Ovali
Michigan Technological University, bovali@mtu.edu

SECOND-LIFE BATTERY ELECTROCHEMICAL IMPEDANCE SPECTROSCOPY MODELING AND APPLICATION TO A RESIDENTIAL SYSTEM

By

Busra Ovali

A REPORT

Submitted in partial fulfillment of the requirements for the degree of

MASTER OF SCIENCE

In Electrical Engineering

MICHIGAN TECHNOLOGICAL UNIVERSITY

2017

This report has been approved in partial fulfillment of the requirements for the Degree of MASTER OF SCIENCE in Electrical Engineering.

Department of Electrical and Computer Engineering

Report Advisor: *Lucia Gauchia*

Committee Member: *Sumit Paudyal*

Committee Member: *Mohsen Azizi*

Department Chair: *Daniel R. Fuhrmann*

Table of Contents

List of Figures

List of Tables

ACKNOWLEDGEMENTS

It is my pleasure to thank all those who made this report possible. I would like to extend my deep sense of gratitude to Dr. Lucia Gauchia for supporting and encouraging me during my research. I could not have completed my research without her assistance. She helped me anytime I needed about my research or my life. I never forget her indescribable guidance and cooperation.

I owe my deepest gratitude to my husband for his invaluable support. He helped and encouraged me anytime when I was desperate. We supported each other during our researches.

I owe special thanks to my family. They always believe that I will be successful and this feeling always gives me encouragement.

ABSTRACT

This study presents the modeling of a used hybrid electric vehicle battery (also called second life battery), and its design and simulation for a standalone residential photovoltaic system. For this purpose, the battery was tested through capacity and electrochemical impedance spectroscopy tests (EIS). These tests were done with variable temperatures (0ºC, 15ºC and 30ºC), and results were used to fit an equivalent impedance circuit. This model was used to incorporate a second life battery to a PV system, which was simulated by using daily irradiance and load data for Tucson (AZ) under most various month (May).

1 INTRODUCTION

Climate changes and resource exhaustion are universal social challenges in present day. Battery technologies are improved nowadays. Their energy storage capacity is an important factor to choose them for electric and electric hybrid automobiles [1]. A normal EV battery lifetime can be 8 or 10 years. Second life EV batteries, that is, batteries repurposed after their EV life has ended in residential or commercial applications can offer lower upfront electric cost [2]. Renewable energy technologies are expected to have a significant role in decreasing these difficulties. Among many renewable technologies, solar photovoltaic (PV) has been found to have a significant potential for electricity generation [3]. PV system uses sunlight directly to produce electricity, so sunny days are more productive and desirable to generate electricity. Also, Photovoltaic (PV) is a clean and sustainable energy where there is no local air pollution and noise during generation [2]. PV system installations have increased recently all around the world because of reducing costs, so it provides an economical way to supply energy needs/ as observed in Figure 1 [4].

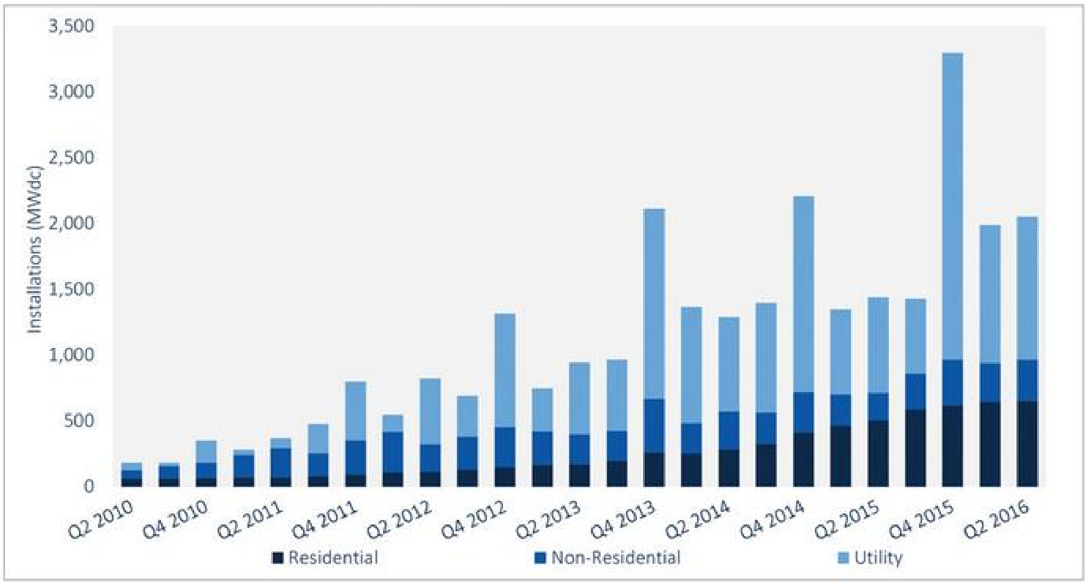

Figure 1 PV installation [5]

Moreover, weather conditions affect power from PV system therefore PV system does not generate electricity in the nights and has reduced production during cloudy days. In these cases, batteries supply the required power[4].

2 TESTS PERFORMED

The objective of this section is to present the battery equivalent circuit model extracted from testing in the laboratory. The tests used are capacity and electrochemical impedance spectroscopy (EIS) is to determine the battery capacity in Amp Hours (Ah), Open Circuit Voltage (OCV) [6], generate Nyquist plots to understand the impedance characteristics for different conditions.

Figure 2 The experimental set up

2.1 CAPACITY TESTING

The battery capacity (Ah) is set by the manufacturer due to the design process, but it is not a fixed value throughout the whole life of the battery. The battery capacity is reduced as the battery ages, and normally follows an Arrhenius equation [10].Capacity tests therefore measure the available capacity in the battery for different operation conditions: variable temperature and battery state-of-charge (SOC). The battery temperature was set using the ESPEC thermal chamber - it controls the environment temperature - , while the SOC for each case was obtained by discharging the battery to the desired SOC level. The procedure was the following, considering the temperature range under study is 0ºC, 15ºC and 30ºC, which are normal battery operation temperatures. The SOC range considered was from 20-80%, which is also the regular SOC window:

1) Thermal chamber was set to 30° C and kept overnight to reach specific temperature at charge to 100 %, 17.75 V MAX, 6 A by using battery tester. (8 h pre-conditioning)
2) Before the testing, the battery OCV is measured.
3) The battery is fully discharged using the NHR battery tester power cycling to charge and discharge batteries- and the Ah discharged were counted. In this case, the voltage setting was 13.2 V at 6.5 A discharge until the current dropped to 0.1. (1 h test)
4) The battery is fully charged using the NHR battery tester again by setting 18.01 V MAX, and 6.51 A to the battery tester. (1 h test)
5) Steps 1-4 are repeated for the rest of temperatures: 0ºC and 15ºC.

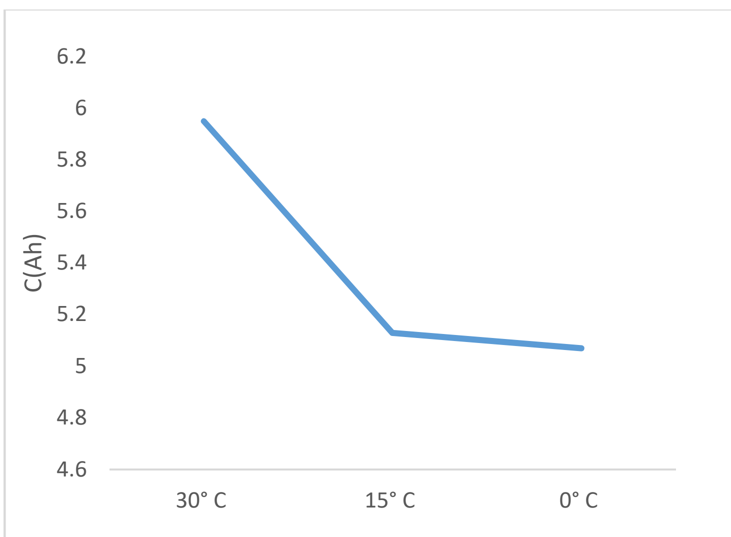

Figure 3 Battery capacity depends on temperature

Results for capacity tests are shown in Figure 3, where it can be observed that the battery capacity decreases with temperature. This effect is expected, as the battery underperforms at lower temperatures due to the change in electrolyte phase that difficult the movements of ions through it.

2.2 ELECTROCHEMICAL IMPEDANCE SPECTROSCOPY (EIS)

EIS testing for batteries allows to experimentally extract the battery complex impedance to be used to model the battery performance [7] . EIS tests are based on the fact that the battery operation can be perturbed by a current or voltage AC signal, small enough to provide linearity in each test. If the AC signal imposed is current it is a galvanostatic test and if it is voltage it is a potentiostatic test. Due to the nature of batteries, it is safer to do a galvanostatic test. Therefore, an AC signal with small amplitude (70mA) was imposed to the battery cells, with a frequency sweep from 3mHz to 1kHz. The choice of frequency is given by the dynamic behavior of batteries, than show a wide frequency window. Also, tests at frequencies lower than 3mHz would increase the testing time and not provide significant information. Once the battery AC signal is imposed to the battery, the voltage will show a ripple due to it, and both are measured by Solartron Modulab – extreme measurement electrochemical test system - which uses them to compute the battery impedance.

The wiring was done through the high voltage module (HV100), as the tested voltage was above the regular 10V accepted. As the battery module tested included two “sticks”, each of them of six cells, the EIS was obtained separately for each stick (auxiliary channels A and B) and for the two together. Wiring is presented in Figure 4, although in our case only Aux. and B were needed. The current imposed to the battery flows through the CE and WE connectors, while the voltage measurement was taken from the RE1 and RE2 connectors.

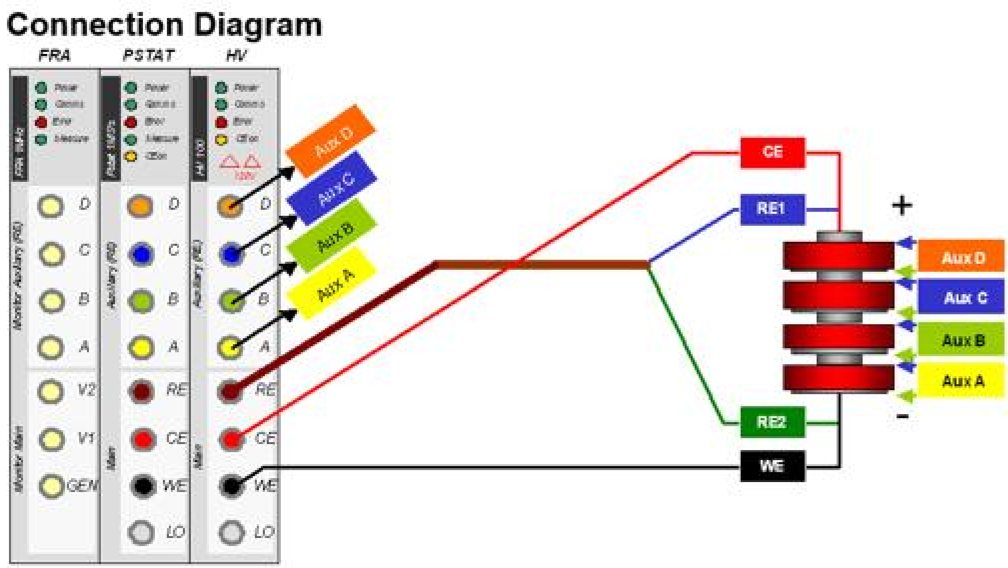

Figure 4 Connection diagram impedance analyzer

The experimental procedure for the electrochemical impedance spectroscopy (EIS) testing is:

1) Temperature of the thermal chamber was set to 30°C and kept overnight to reach specific temperature. (8h pre-conditioning)
2) The battery was 20% discharged and state of charge (SOC) was reached at 80%. (15min test plus 30 min resting)
3) The battery tester was disconnected and the impedance analyzer was connected the battery.
4) The battery OCV was measured using the impedance analyzer.

5) EIS test was done through the Solartron Modulab equipment–electrochemical test system -. Data was stored for later processing. (2h15min test)
6) After the EIS testing, the impedance analyzer wiring was removed and battery tester was connected.
7) The state of charge (SOC) was reduced 20% and SOC was set 60%. (15 min test plus 30 min resting)
8) The same procedure from 3-6 was carried out for 60%, 40%, 20%.
9) After the 20% SOC EIS testing, the battery was fully charged. The temperature of the thermal chamber was set to 15° C and kept overnight.
10) The same process from 1-9 was repeated for 15° C and 0° C.

2.3 EIS RESULTS

This section shows the results obtained from the EIS testing presented above. The objective of this section is to model the battery through an electrical equivalent circuit that translates electrochemical phenomena into electrical components.

It was possible to detect the component values from battery equivalent circuit by testing the full frequency response of the battery pack and then implementing a fitting process to data. The Nyquist plots presented below were obtained for four different state of charge (SOC) at three different temperatures (0º, 15º and 30º). The figures below show three curves, one for Aux A (one stick that is composed by 6 cells), Aux B (the other stick in the module, also with 6 cells) and the total impedance Z which represents the addition of Aux A and B. Fitting for the total Z is also presented.

As it can be observed, even in Aux A and B are seemingly identical systems, they present different impedance spectra. For example, in the first curve, Aux. B presents a resonance impedance (cross at Z=0) that is a 48% larger than Aux. A. This is an important information as it shows that individual cells in the same battery pack present different impedance and aging performance.

Results shown that the Aux A impedance is consistently larger than Aux B, except for a single test at 0ºC and 40% SOC, where both spectras were below a 5% difference among them. There is another case at 15ºC 40% SOC where Aux B presents a highly noisy and not readable spectra that will require repetition of the test.

This graph presented below shows each part of the Nyquist plot means. R1 represents equivalent series resistance of the battery. It can be evaluated between Nyquist curve and x axis. Each parallel circuit of capacitance (CPE1, CPE2) and resistance (R2, R3) correspond the semi-circle in the Nyquist diagram and represent the dynamic behavior of the electrode/electrolyte interface [8].

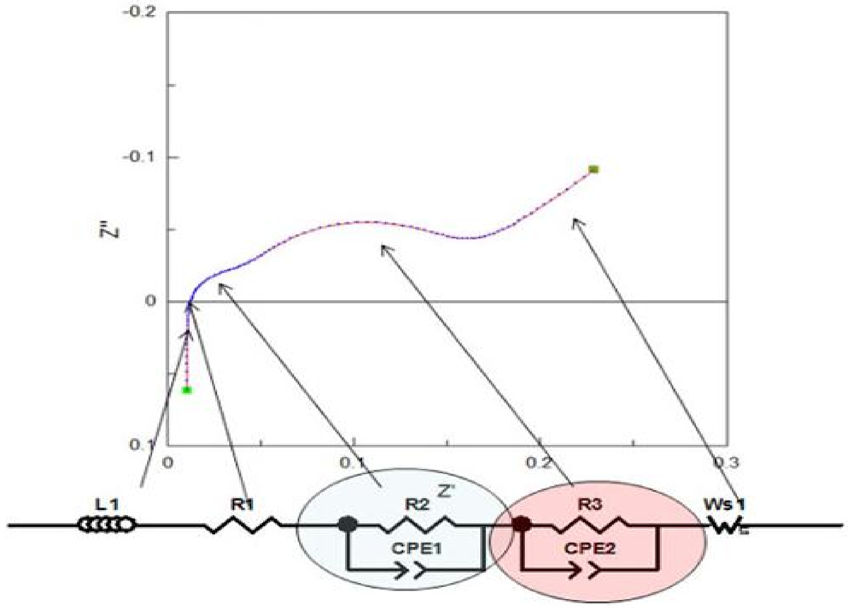

Figure 5 The circuit elements corresponding to the features in the EIS plots [9]

The Nyquist plots presented below were obtained for four different state of charge (SOC) and only 30°C equations were used to obtain these plots.

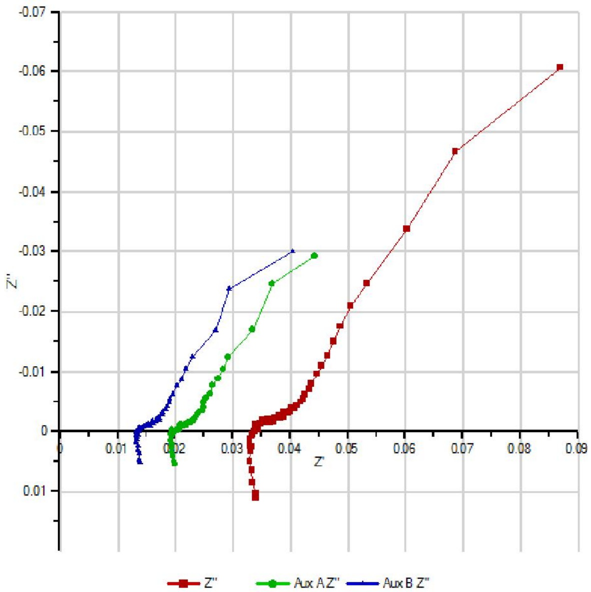

Figure 6 Nyquist plot with Aux A, B, total for 20% SOC at 30° C

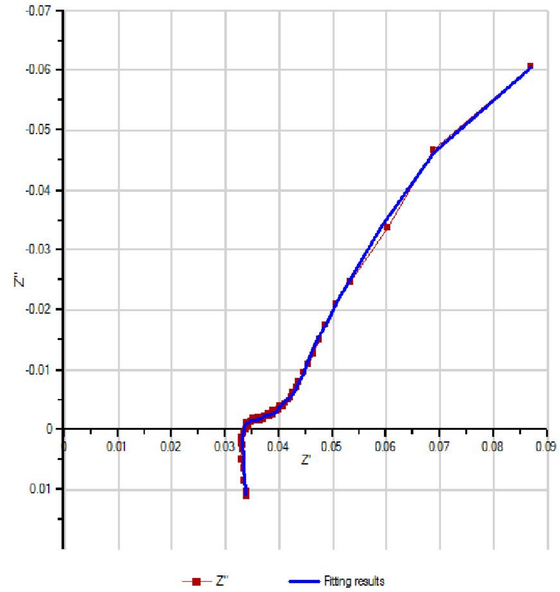

Figure 7 Nyquist plot with fitting result for 20% SOC at 30° C

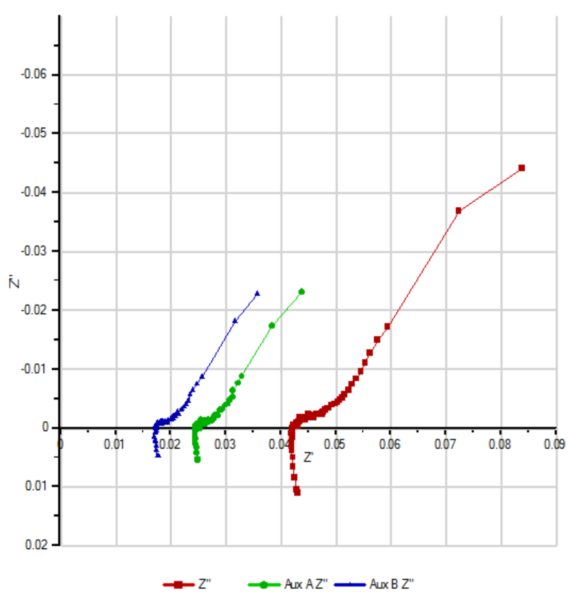

Figure 8 Nyquist plot with Aux A, B, total for 40% SOC at 30° C

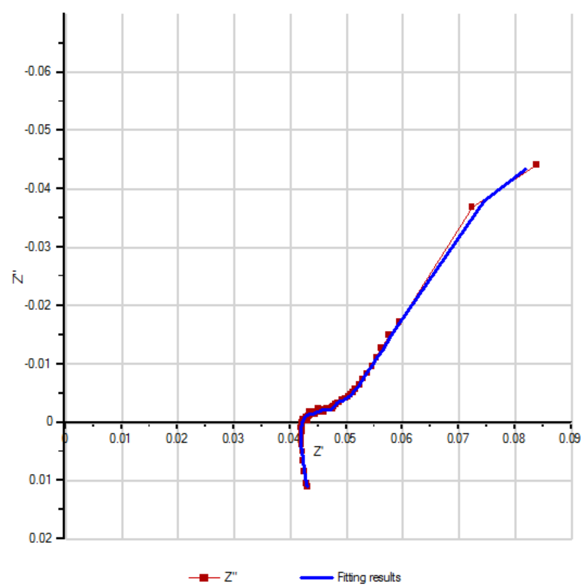

Figure 9 Nyquist plot with fitting result for 40% SOC at 30° C

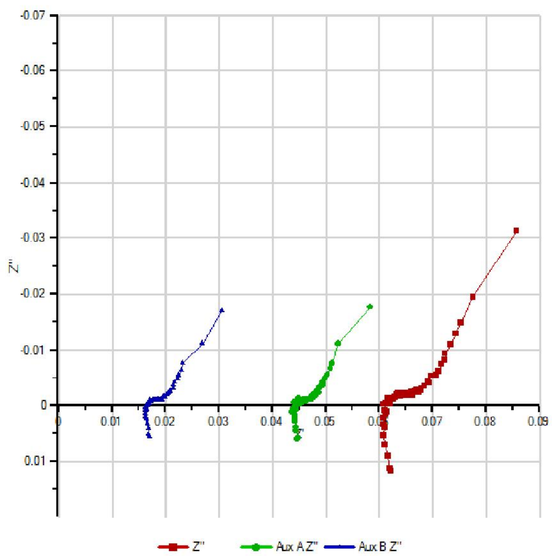

Figure 10 Nyquist plot with Aux A, B, total for 60%SOC at 30° C

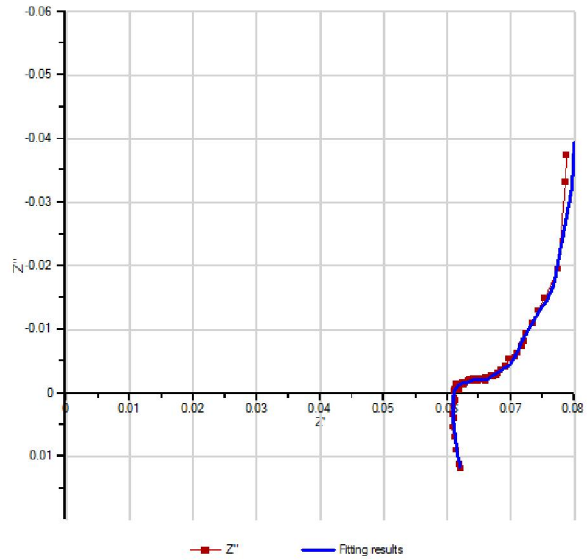

Figure 11 Nyquist plot with fitting result for 60% SOC at 30° C

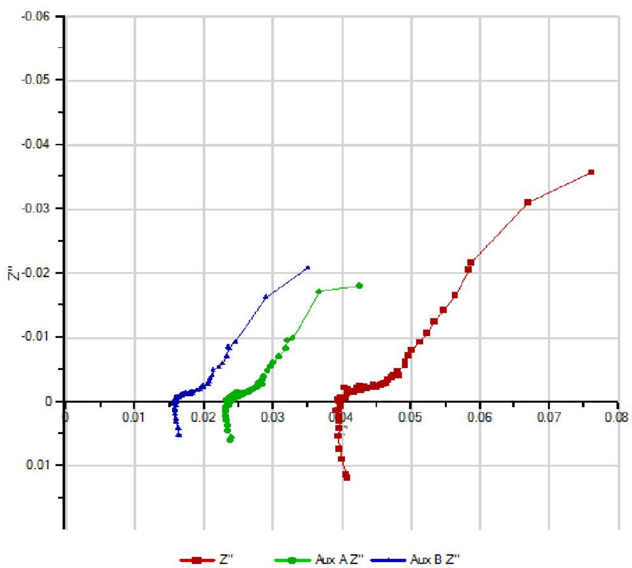

Figure 12 Nyquist plot with Aux A, B, total for 80% SOC at 30° C

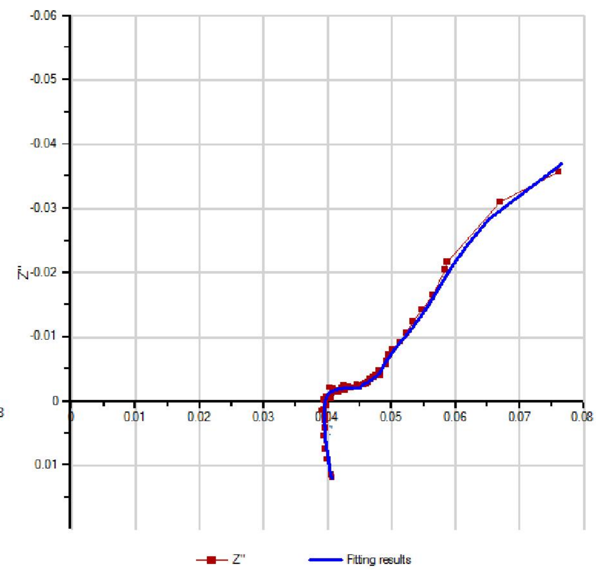

Figure 13Nyquist plot with fitting result for 80% SOC at 30° C

3 BATTERY

Nowadays there is a wide range of battery technologies. These variations depend on the requirements and applications [9]. A nickel–metal hydride battery (NiMH or Ni-MH) is a rechargeable battery. NiMH batteries are used in Honda Civic hybrid electric vehicle. NiMH battery energy density nearly equals lithium-ion battery [11].

3.1 MATHEMATICAL MODEL OF BATTERY

The battery cell equivalent circuit given in Figure 14 was created to obtain fitting results. This battery model has one series resistor, five resistor-capacitor (RC) parallel network and one resistor-inductor (RL) parallel network. The series resistor R_0 represents the lumped contact resistances and electrolyte impedance. The RC networks provide the dynamic performance of the battery by presenting different time constants (one for each RC) which reproduce the faster double layer dynamics in the electrode-electrolyte interface and the slower dynamics of mass transfer along the electrolyte. These phenomena can also be modeled through electrochemical elements such as Warburg, but as it does not have an electrical nature, it cannot be included as such. The Warburg element is typically electrically represented as a concatenation of RC networks, so the circuit shown does represent the phenomena taking place. The RL network is due to the increase of impedance at higher frequencies as the electrical collectors reduce the active surface to the skin. Therefore, this RL does not represent electrochemical phenomena, but material resistance change at high frequencies.

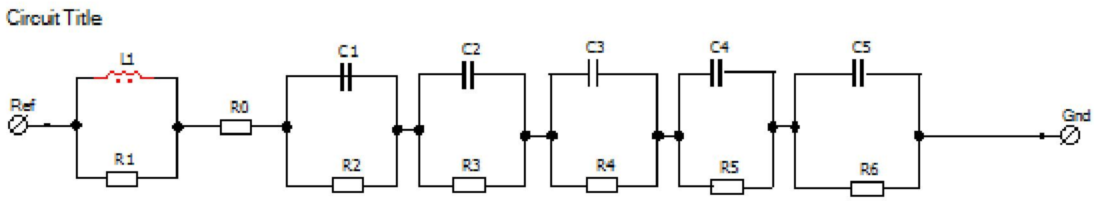

Figure 14 Battery cell equivalent circuit

The battery circuit is a function the temperature and SOC, as shown in Table 1.

Temp	SOC	L1 (mH)	R1 (Ohm)	R0(Ohm)	R2(Ohm)	C1 (F)	R3(Ohm)	C2(F)	R4(Ohm)	C3(F)	R5(Ohm)	C4(F)	R6(Ohm)	C5(F)
30	20	0.00176	0.2045	0.03332	0.00287	2.188	0.003078	26.96	0.00449	221.9	0.1369	696.1	0.01132	957
30	40	0.0018	0.1068	0.04189	0.00258	1.644	0.002924	17.31	0.00428	174.8	0.1004	966.1	0.00728	990.2
30	60	0.00192	0.11276	0.06085	0.00231	1.9247	0.002834	13.743	0.00323	154.35	0.0892	931.81	0.00438	957.7
30	80	0.00195	0.1214	0.03945	0.00279	2.373	0.002848	20.13	0.00302	212.9	0.08218	1107	0.00773	875.1
15	20	0.00179	0.1783	0.05322	0.00371	1.48	0.005441	11.48	0.00593	125.7	0.1289	613.5	0.01094	682
15	40	0.00185	0.1013	0.04246	0.00346	1.523	0.005745	11.07	0.00557	137.1	0.112	850.8	0.00858	824.5
15	60	0.00187	0.1625	0.04774	0.00347	2.151	0.006354	12.13	0.00551	159	0.1334	963.4	0.01015	973.2
15	80	0.00185	0.1543	0.03139	0.00362	2.067	0.006791	11.51	0.00524	188.5	0.1679	1226	0.02002	879.4
0	20	0.00169	0.8098	0.0411	0.00486	1.161	0.009831	7.192	0.00931	53.48	0.01102	460.2	0.1408	594.5
0	40	0.00181	0.4243	0.03496	0.0039	1.951	0.009722	7.963	0.0088	52.92	0.01086	385.6	0.1131	744.8
0	60	0.00178	0.411	0.04386	0.00523	2.143	0.01333	9.604	0.00922	108.6	0.01306	879.2	0.2731	868
0	80	0.00182	0.1549	0.03288	0.00324	1.257	0.009918	6.203	0.01217	28.57	0.00903	433.6	0.115	691.8

Table 1 Fitting results

3.2 BATTERY SIMULATION

Battery model is designed in Simulink for this study. These following equations were used to develop this system. These equations were calculated for three temperature (30°C, 15° C and 0° C).

These equations are for 30°C:

$$R_2=0.0001*SOC^3-0.0007*SOC^2+0.001*SOC+0.0024 \quad (1)$$

$$C_1=-0.1095*SOC^3-1.0694*SOC^2+2.9857*SOC+4.2138 \quad (2)$$

$$R_3\text{=0.000000.7*}SOC^3\text{-0.00001*}SOC^2\text{-0.0002* }SOC\text{+0.0033} \quad (3)$$

$$C_2\text{=0.6452*}SOC^3\text{-0.829*}SOC^2\text{-11.678* }SOC\text{+38.822} \quad (4)$$

$$R_4\text{=0.0003*}SOC^3\text{-0.0021*}SOC^2\text{+0.0042* }SOC\text{+0.0021} \quad (5)$$

$$C_3\text{=8.725*}SOC^3\text{-39.025*}SOC^2\text{+8.9* }SOC\text{+243.3} \quad (6)$$

$$R_5\text{=-0.0035*}SOC^3\text{+0.0338*}SOC^2\text{-0.1131* }SOC\text{+0.2198} \quad (7)$$

$$C_4\text{=0.0107*}SOC^3\text{-1.6648*}SOC^2\text{+83.417* }SOC\text{-391.66} \quad (8)$$

$$R_6\text{=0.0009*}SOC^3\text{-0.0045*}SOC^2\text{+0.0036* }SOC\text{+0.0114} \quad (9)$$

$$C_5\text{=2.595*}SOC^3\text{-48.415*}SOC^2\text{+160.28* }SOC\text{+842.54} \quad (10)$$

These equations are for 15° C:

$$R_2\text{=-0.00002*}SOC^3\text{+0.0002*}SOC^2\text{-0.0008* }SOC\text{+0.0043} \quad (11)$$

$$C_1\text{=-0.2162*}SOC^3\text{+1.5895*}SOC^2\text{-3.2123* }SOC\text{+3.319} \quad (12)$$

$$R_3\text{=-0.00008*}SOC^3\text{+0.0006*}SOC^2\text{-0.001* }SOC\text{+0.0059} \quad (13)$$

$$C_2\text{=-0.525*}SOC^3\text{-+3.885*}SOC^2\text{-8.39* }SOC\text{+16.51} \quad (14)$$

$$R_4\text{=-0.00009*}SOC^3\text{+0.0007*}SOC^2\text{-0.0018* }SOC\text{+0.0071} \quad (15)$$

$$C_3\text{=-0.4833*}SOC^3\text{+8.15*}SOC^2\text{-9.6667* }SOC\text{+127.7} \quad (16)$$

$$R_5\text{=-0.0042*}SOC^3\text{+0.044*}SOC^2\text{-0.1265* }SOC\text{+0.2093} \quad (17)$$

$$C_4\text{=-0.0057*}SOC^3\text{-0.8426*}SOC^2\text{+46.398* }SOC\text{-23.2} \quad (18)$$

$$R_6\text{=0.0007*}SOC^3\text{-0.0024*}SOC^2\text{-0.0003* }SOC\text{+0.0129} \quad (19)$$

$$C_5\text{=-41.45*}SOC^3\text{+251.8*}SOC^2\text{-322.75* }SOC\text{+794.4} \quad (20)$$

These equations are for 0° C:

$$R_2\text{=-0.0009*}SOC^3\text{+0.0067*}SOC^2\text{-0.0147* }SOC\text{+0.0137} \quad (21)$$

$$C_1\text{=-0.08*}SOC^3\text{+0.181*}SOC^2\text{+0.807* }SOC\text{+0.253} \quad (22)$$

$$R_3\text{=-0.0018*}SOC^3\text{+0.0126*}SOC^2\text{-0.0254* }SOC\text{+0.0244} \quad (23)$$

$$C_2\text{=-0.9853*}SOC^3\text{+6.347*}SOC^2\text{-11.373* }SOC\text{+13.203} \quad (24)$$

$$R_4\text{=0.0003*}SOC^3\text{-0.0012*}SOC^2\text{+0.0011* }SOC\text{+0.0091} \quad (25)$$

$$C_3\text{=-31.992*}SOC^3\text{+220.07*}SOC^2\text{-436.83* }SOC\text{+302.23} \quad (26)$$

$$R_5\text{=-0.0014*}SOC^3\text{+0.0098*}SOC^2\text{-0.0195* }SOC\text{+0.0221} \quad (27)$$

$$C_4\text{=-251.23*}SOC^3\text{+1791.5*}SOC^2\text{-3690.5* }SOC\text{+2610.4} \quad (28)$$

$$R_6\text{=-0.0843*}SOC^3\text{+0.5996*}SOC^2\text{-1.2365* }SOC\text{+0.862} \quad (29)$$

$$C_5\text{=-45.383*}SOC^3\text{+258.75*}SOC^2\text{-308.27* }SOC\text{+689.4} \quad (30)$$

4 RESIDENTAL PV SYSTEM

Photovoltaic (PV) systems convert solar light to electricity directly in the stand-alone mode, the PV/storage system can be or not decoupled from the electric distribution grid , in off-grid and grid-connected modes [5].

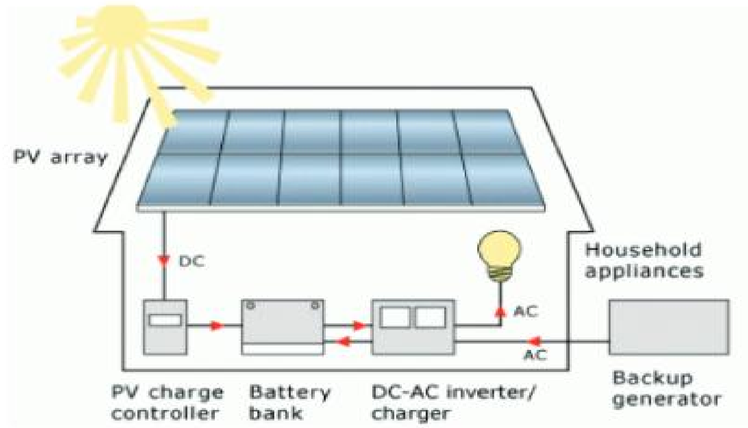

Figure 15 PV System [10]

The pv array, maximum power point tracking (MPPT) control, battery, charge controller, and inverter are the components of a PV systems, as shown in Figure 15 [6], [7].PV generation operates when solar irradiation impact the PV panels, and these panels convert solar radiation into electrical energy and convey it to the rest of the system to be consumed by the load or stored by the batteries. The batteries are used to store energy when the demand is lower than energy producedor when the demand is higher than the power generated by the PV. This energy is used during night time and during cloudy weather conditions which present reduced solar radiation [8].

There are six subystem in this system. They are PV model, battery charge controller, MPPT, dc-dc converter, and battery as shown in Figure 16.

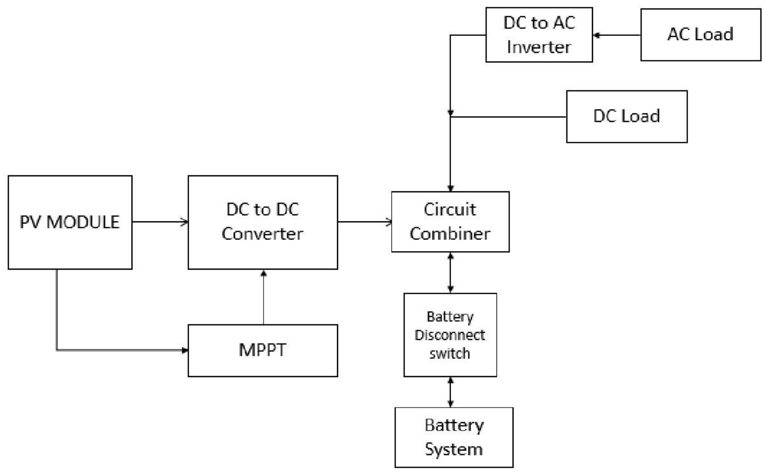

Figure 16 Structure of PV Residential System

4.1 MATHEMATICAL MODEL OF PV SYSTEM

An electrical circuit that combines the solar irradiation, p-n junction and losses represents the PV model, as shown in Figure 17. The solar irradiation is modeled by a current source, while an anti-parallel diode represent the Si p-n junction. The series and parallel resistance represents the ohmic losses and internal losses [5]. The equations for the PV panel model are presented below.

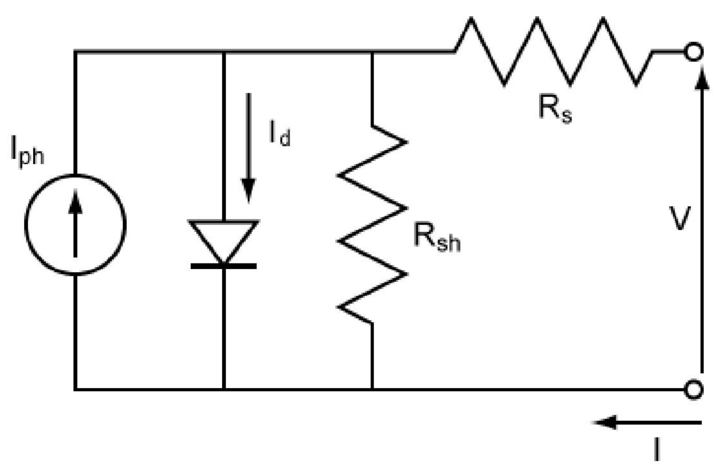

Figure 17 PV Equivalent Circuit [11]

The current is calculated by using following equation. I_{ph} is the Photocurrent, I_d is the diode current, I_P is the parallel current.

$$I = I_{ph} - I_d - I_P \tag{31}$$

I_0 is the saturation current, V_T is the thermal voltage, R_s is the serial resistance

$$V_T = k\,.T_c/q \tag{32}$$

V_T is the thermal voltage, q is the electron charge constant, T_c is the actual cell temperature

$$I_{ph} = \frac{G}{G_{ref}}\left(I_{ph,ref} + \mu_{sc}.\varDelta T\right) \tag{33}$$

G is the irradiance**,** G_{ref} is the irradiance at standard test condition(STC) (1000 $W/_{m^2}$), $I_{ph,ref}$ is photo current at STC, μ_{sc} the coefficient temperature for the short circuit current.

$$\varDelta T = T_c - T_{c,ref} \tag{34}$$

$T_{c,ref}$ is the cell temperature at STC.

$$I_P = \frac{\mathrm{V} + R_s.I}{R_p} \tag{35}$$

R_p is the parallel resistance for internal losses in equivalent circuit.

Therefore, the general equation of the PV system is:

$$I = \frac{G}{G_{ref}}\left(I_{ph,ref} + \mu_{sc}.\Delta T\right) - I_0\left[e^{\frac{V+I.R_S}{a}} - 1\right] - \frac{V + R_S.I}{R_p} \tag{35}$$

5 SYSTEM SIZING:

5.1 PV SIZING

The PV sizing used in this M.Sc. is the result from the M.Sc. titled “Design and Simulation of a Residential PV-Battery System”, by Sevket Burak Ovali. The PV module has 36 cells and each cell produce 0.6V. The open circuit voltage (V_{oc}) is 21.1V. The short circuit current (I_{sc}) is 3.74 A. The voltage at maximum power (V_m) is 3.479 V. The current at maximum power (I_m) is 17.45 A. The maximum power (P_m) is 60.7 W. The actual rated array is calculated by multiplying the module rated maximum power by the total number of modules. For Tucson, the module has a rated maximum power of 60.7 W, the total number of modules is 66, and actual array rated power is 40006.2 W.

5.2 BATTERY SIZING

The battery cell has 6.5 Ah capacity. The maximum allowed depths of discharge (DOD) is 80% and the battery efficiency is 0.85 in this study. The battery pack rated capacity (B_{rated}) is 1637 Ah for Tucson. The energy demand is 20950 Wh/day and autonomy days is 3 for Tucson.

6 RESULT AND DISCUSSION

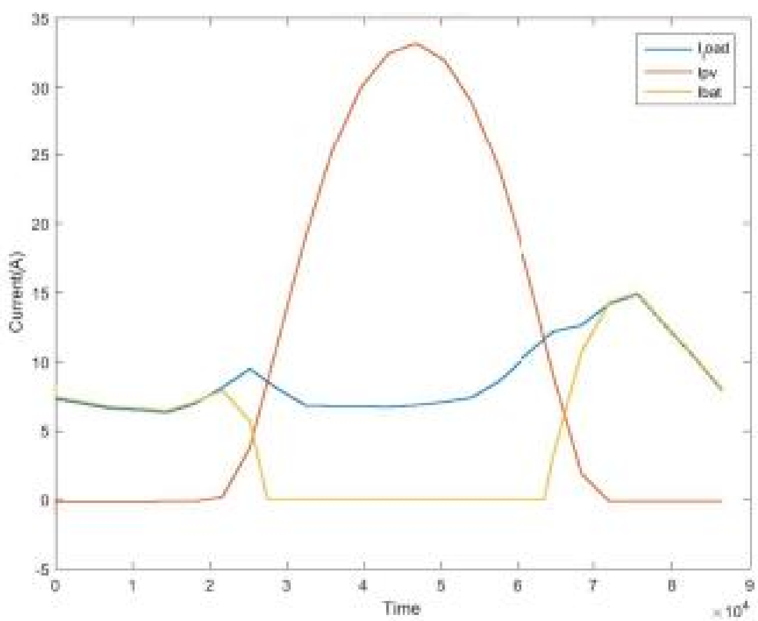

Figure 18 First day currents for Tucson(May 1)

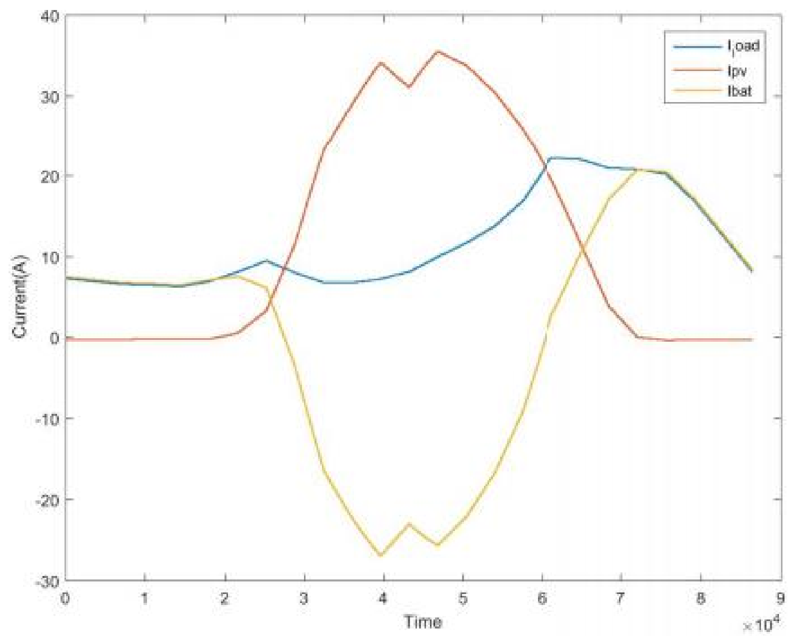

Figure 19 Last day currents for Tucson(May 31)

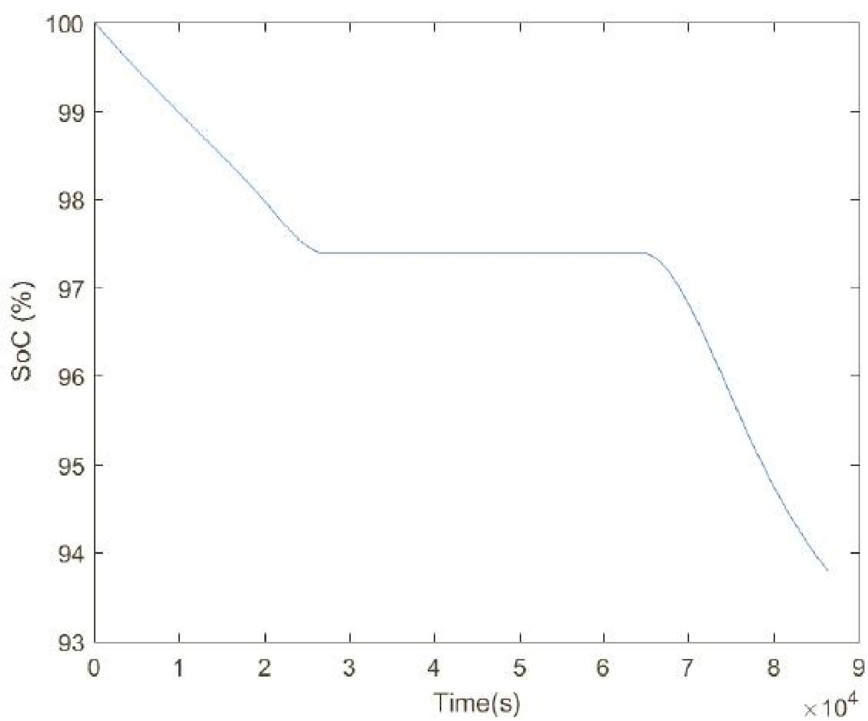

Figure 20 First day SoC for Tucson(May 1)

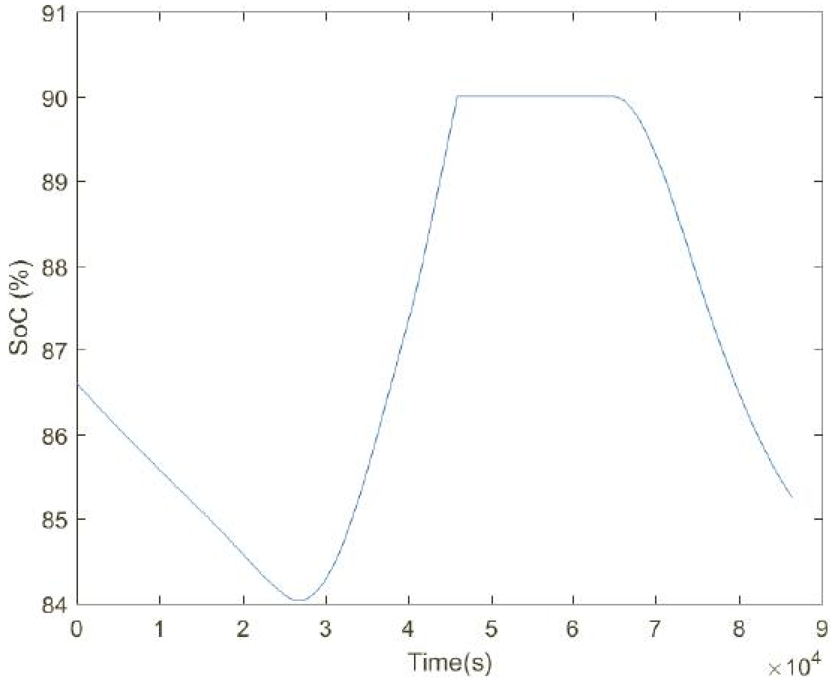

Figure 21 Last day SoC for Tucson(May 31)

The daily solar irradiation can be changed depends on climates or location. In this study, Arizona was simulated based on May. State of charge (SOC) is assumed to be 100% at the beginning of the month. First day and last day of SOC results are given above. When the battery reaches full charge, the SOC reaches to 90%. Battery should be protected against the over discharge/charge so SOC is kept between 20% and 90%.

Figure 18 shows that PV generates sufficient electricity for load and battery at the beginning of the May. Also Figure 21 represents that SOC was decreasing but sometimes it was stable based on charge controller. When the battery current is going to negative side (Figure 19), the battery SOC is rising, that means, PV system begins to charge the battery.

In some sunny days, when the battery is fully charged with 90% SOC, the power generated from PV system is more than load demand. Our PV system doesn't connect grid, but if it would, then the cost of PV system can be reduced because in some sunny days, it can sell it back to the grid.

7 APPENDICES

The Nyquist plots presented below were obtained for four different state of charge (SOC) at 15° C temperature.

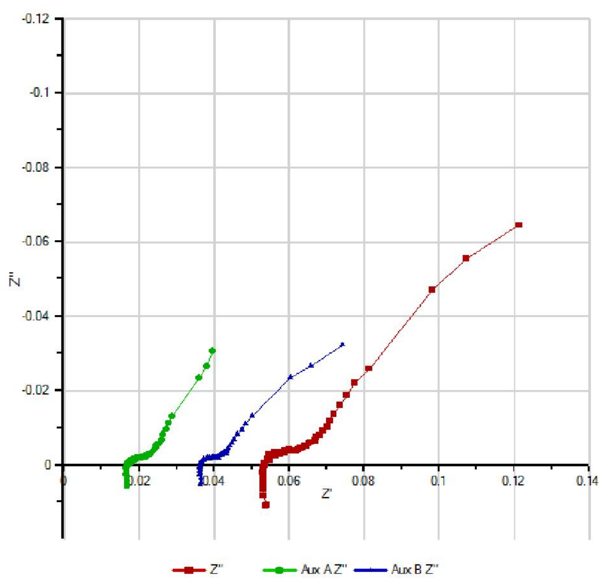

Figure 22 Nyquist plot with Aux A, B, total for 20% SOC at 15° C

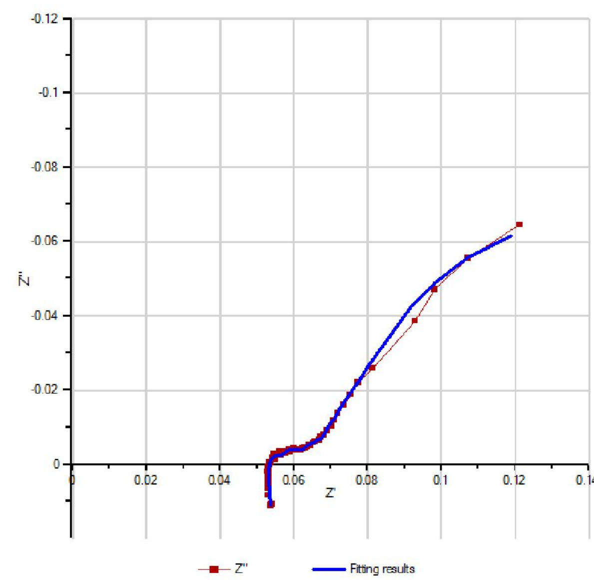

Figure 23 Nyquist plot with fitting result for 20% SOC at 15° C

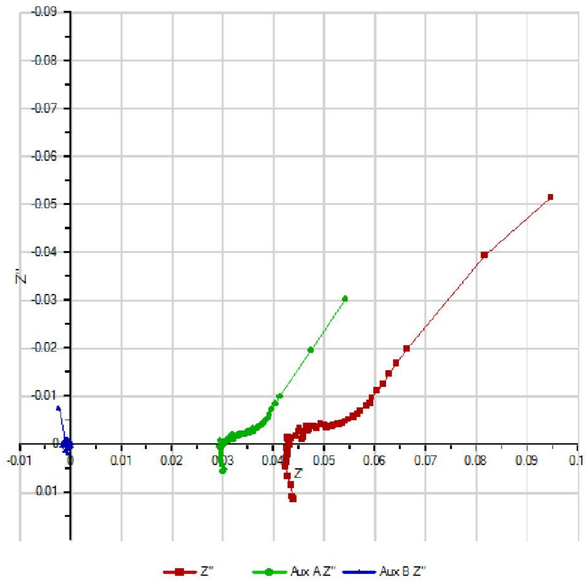

Figure 24 Nyquist plot with Aux A, B, total for 40% SOC at 15° C

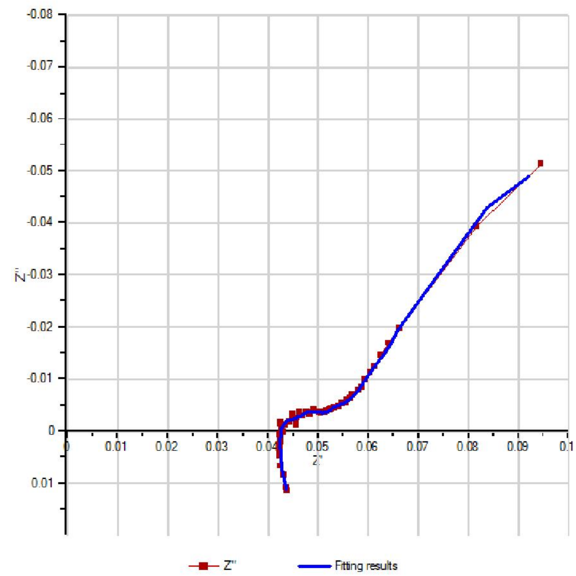

Figure 25 Nyquist plot with fitting result for 40% SOC at 15° C

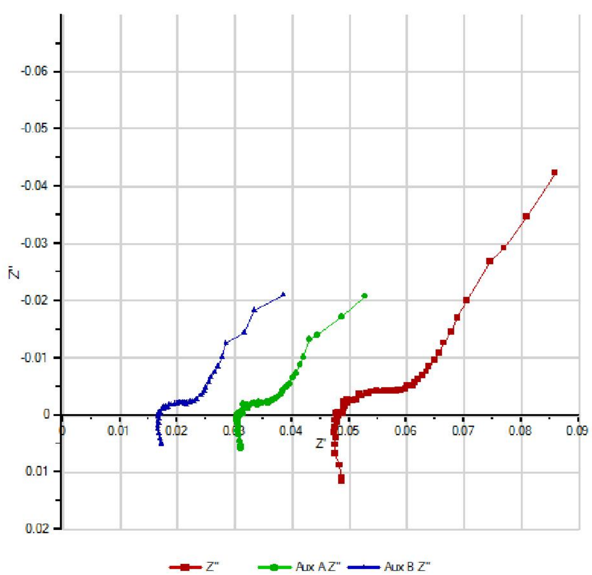

Figure 26 Nyquist plot with Aux A, B, total for 60% SOC at 15° C

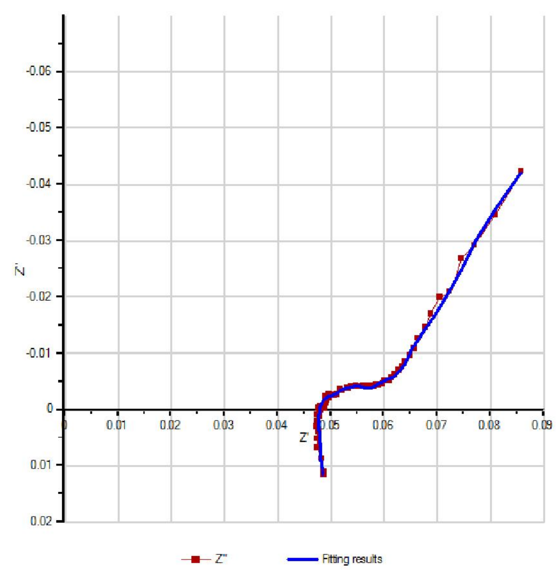

Figure 27 Nyquist plot with fitting result for 60% SOC at 15° C

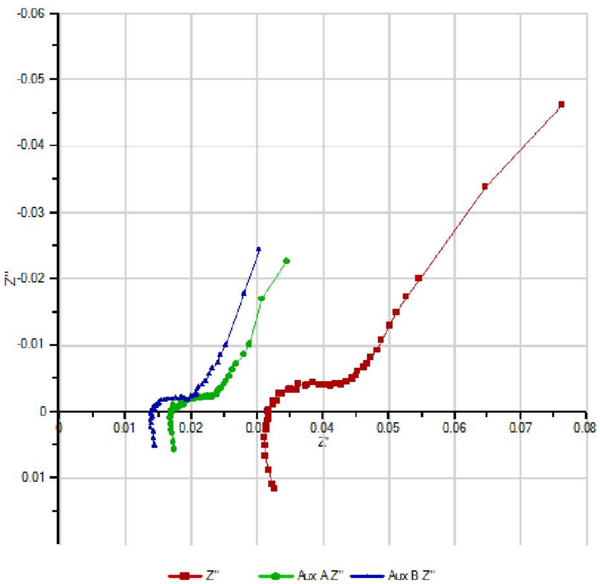

Figure 28 Nyquist plot with Aux A, B, total for 80% SOC at 15° C

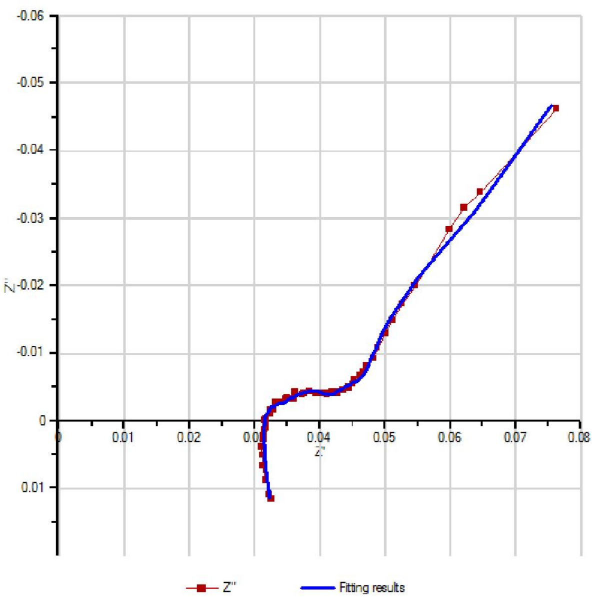

Figure 29 Nyquist plot with fitting result for 80% SOC at 15° C

The Nyquist plots presented below were obtained for four different state of charge (SOC) at 0° C temperature.

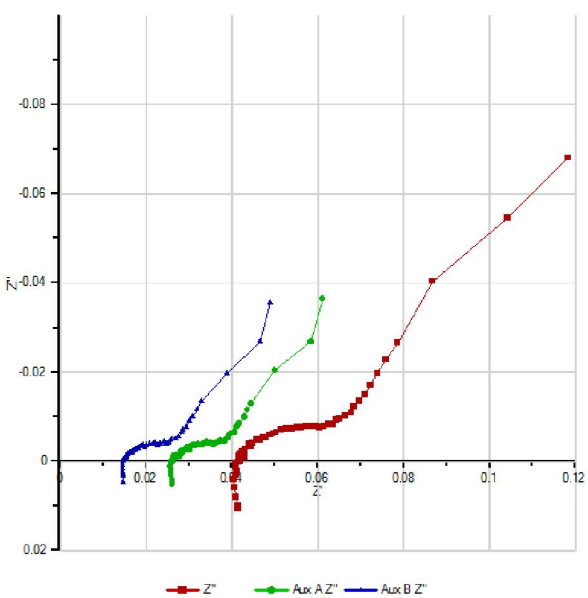

Figure 30 Nyquist plot with Aux A, B, total for 20% SOC at 0° C

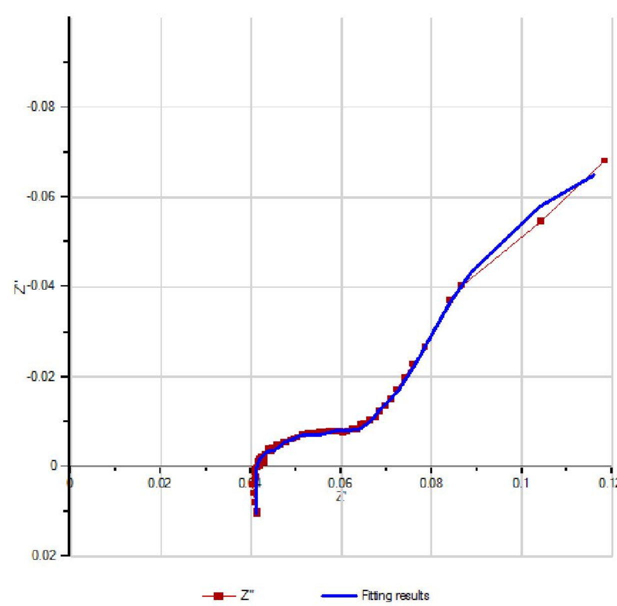

Figure 31 Nyquist plot with fitting result for 20% SOC at 0° C

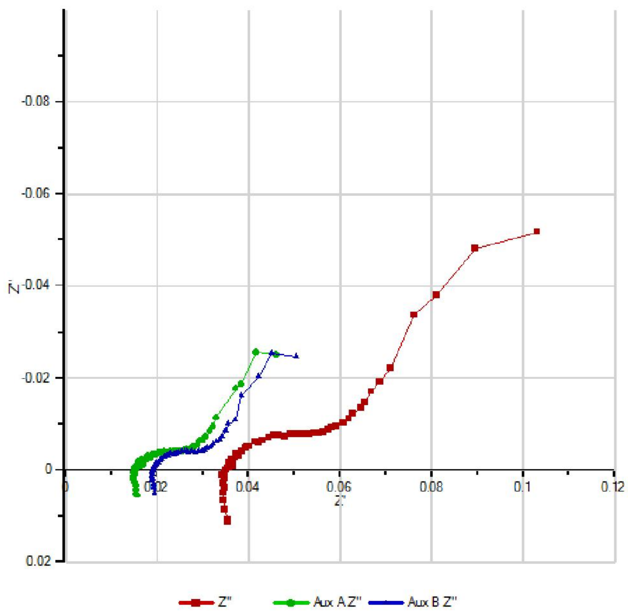

Figure 32 Nyquist plot with Aux A, B, total for 40% SOC at 0° C

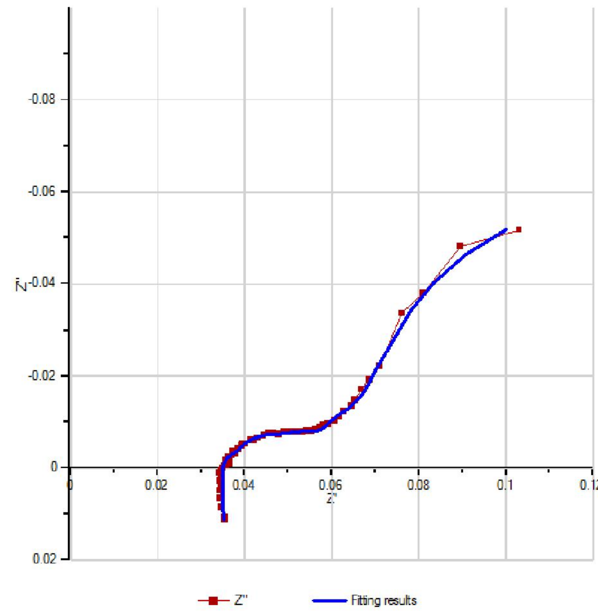

Figure 33 Nyquist plot with fitting result for 40% SOC at 0° C

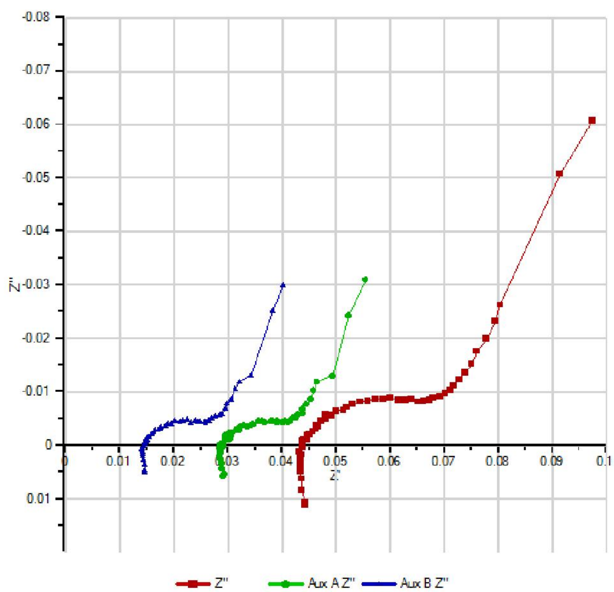

Figure 34 Nyquist plot with Aux A, B, total for 60% SOC at 0° C

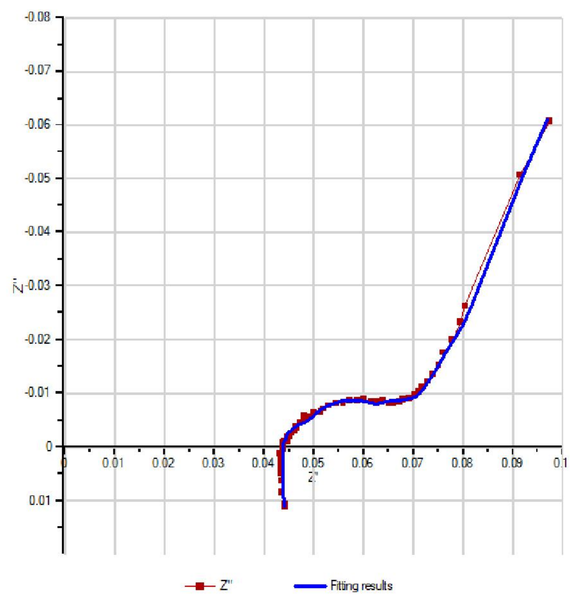

Figure 35 Nyquist plot with fitting result for 60% SOC at 0° C

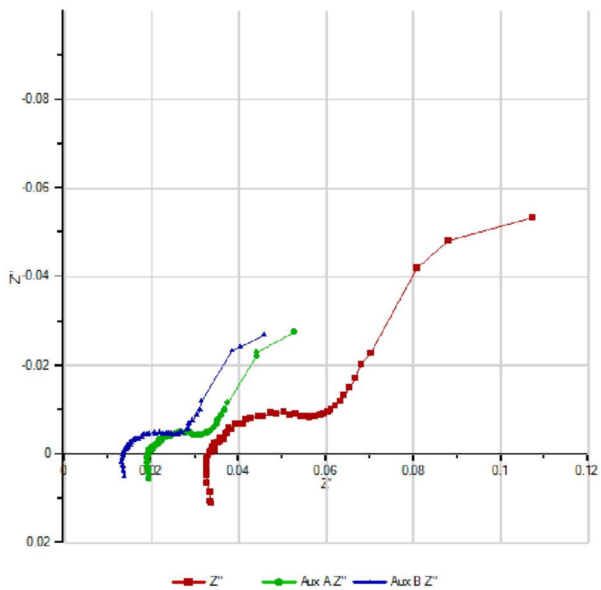

Figure 36 Nyquist plot with Aux A, B, total for 80% SOC at 0° C

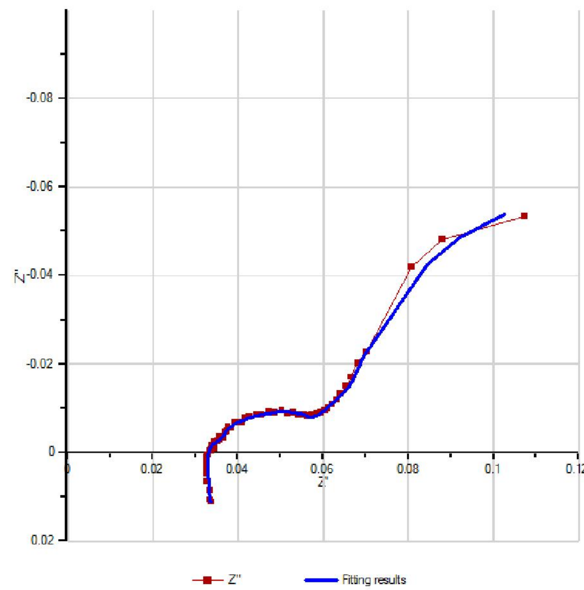

Figure 37 Nyquist plot with fitting result for 80% SOC at 0° C

Simulation Results for May in Tucson

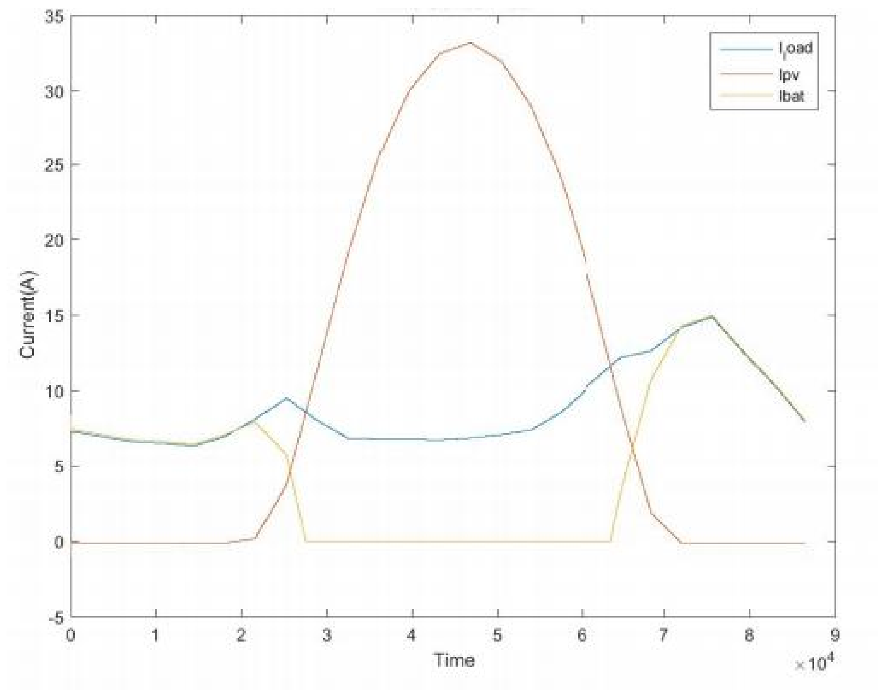

Figure 38 May 1

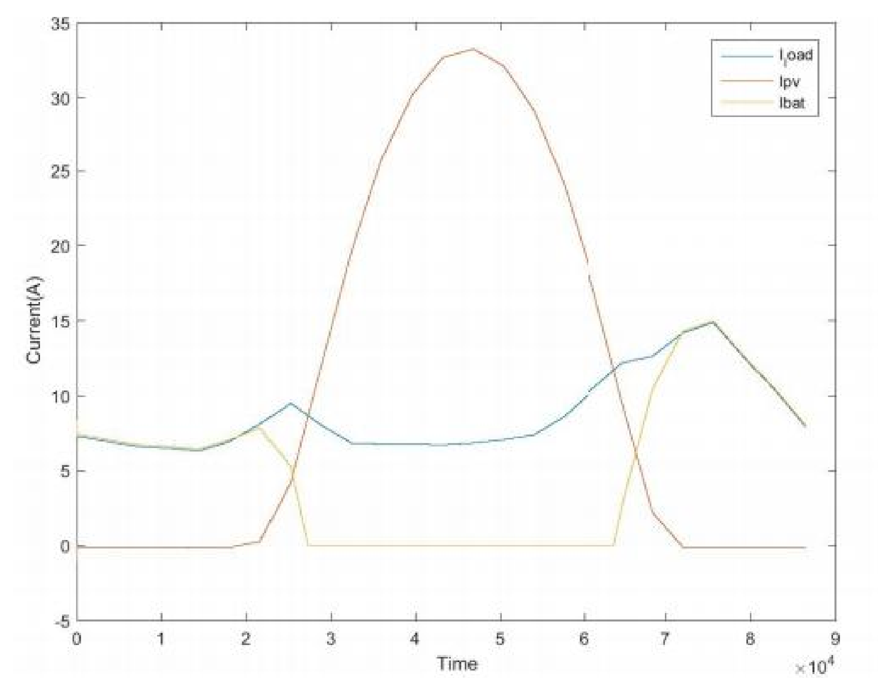

Figure 39 May2

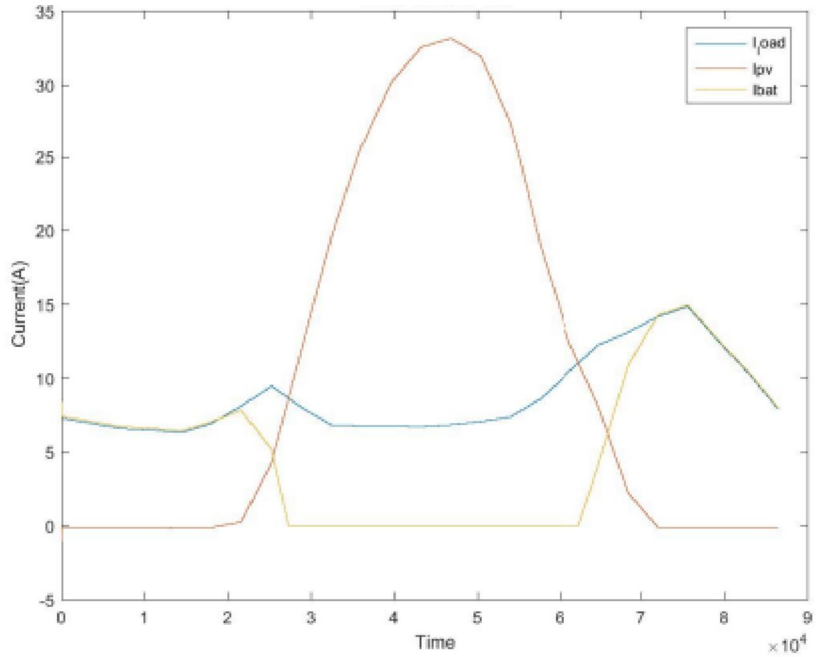

Figure 40 May3

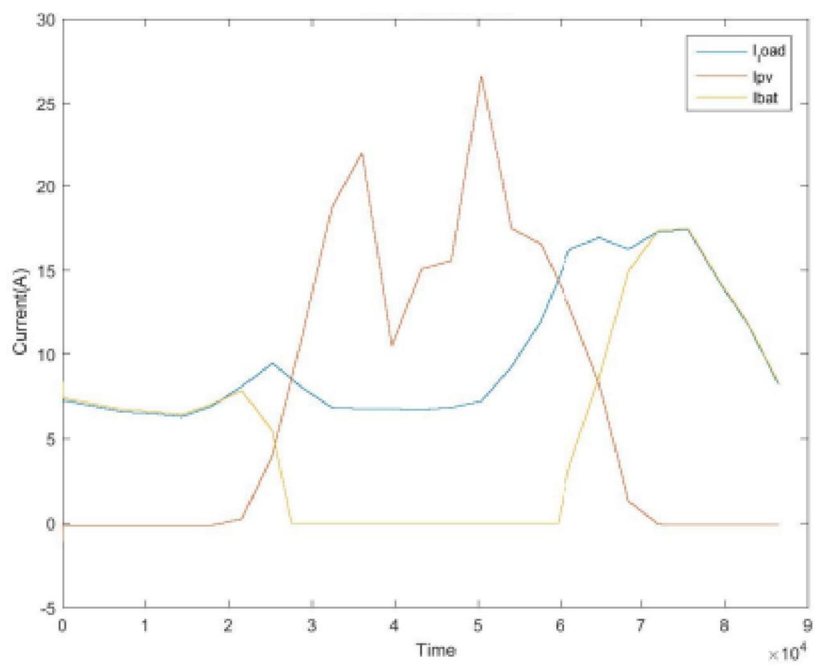

Figure 41 May4

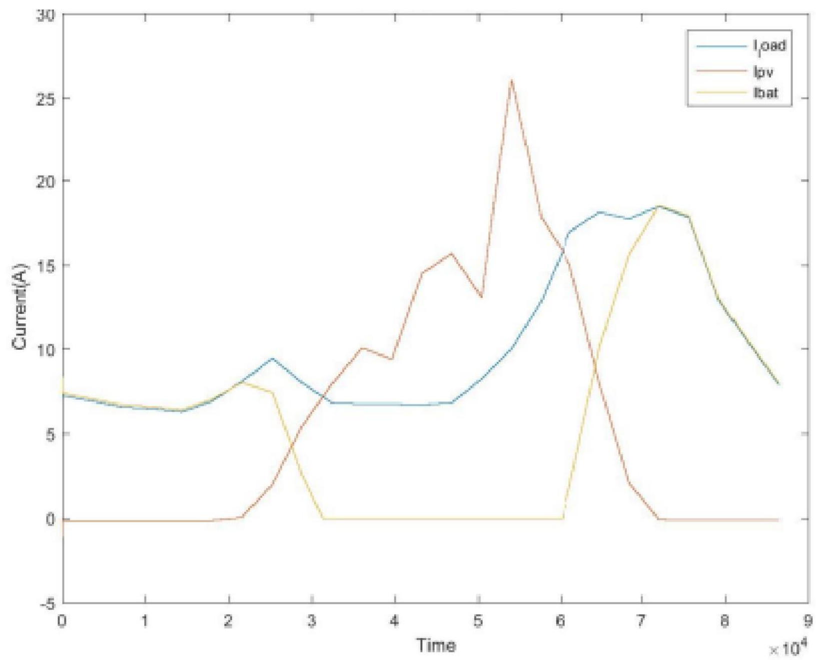

Figure 42 May5

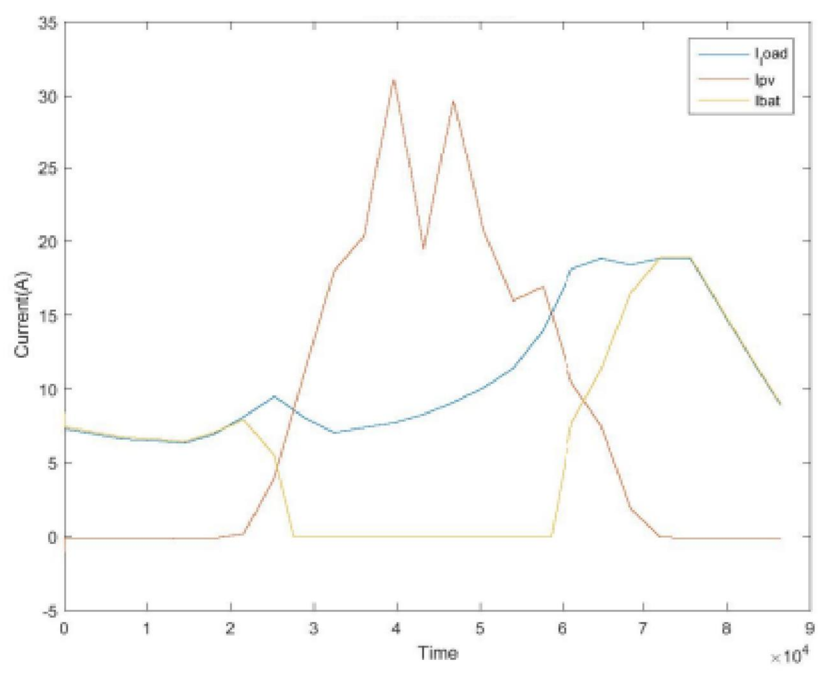

Figure 43 May6

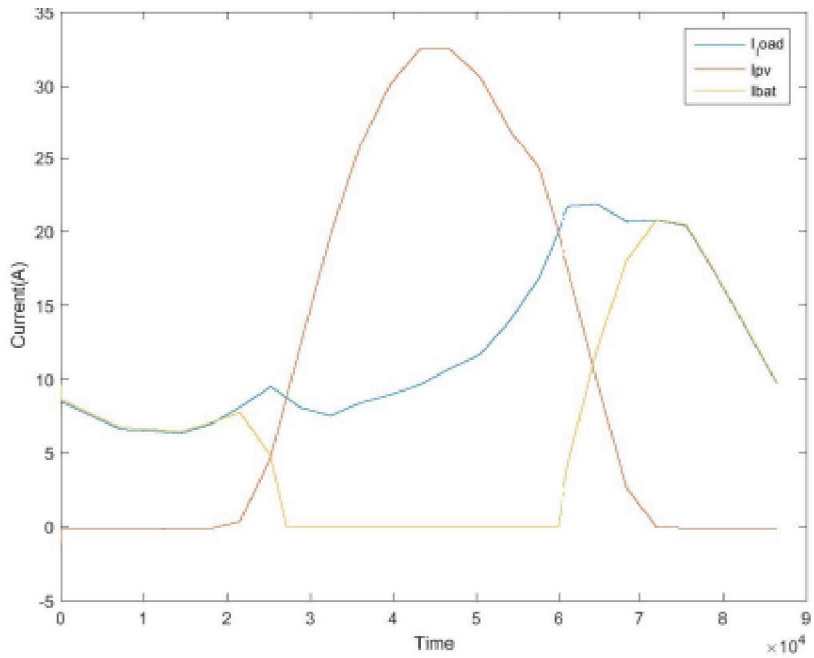

Figure 44 May7

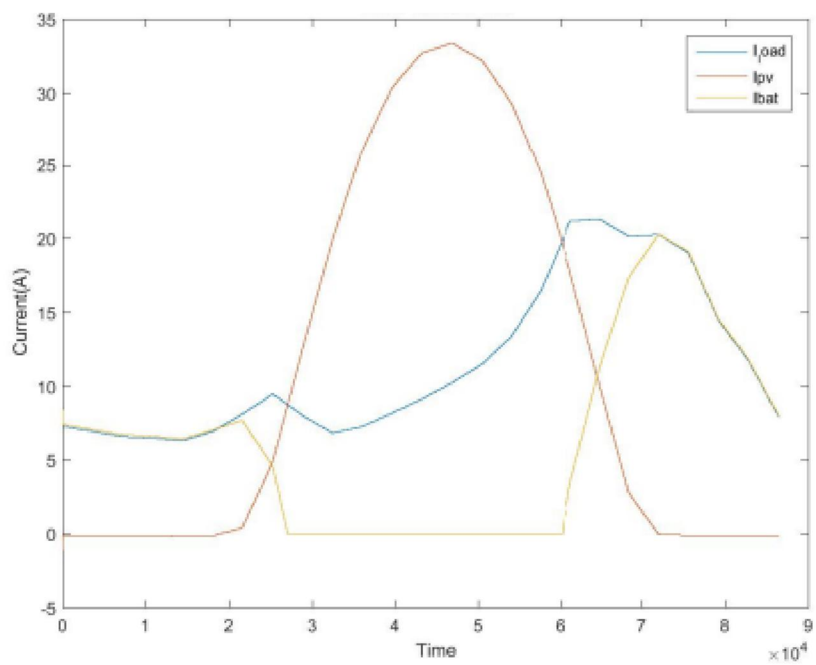

Figure 45 May8

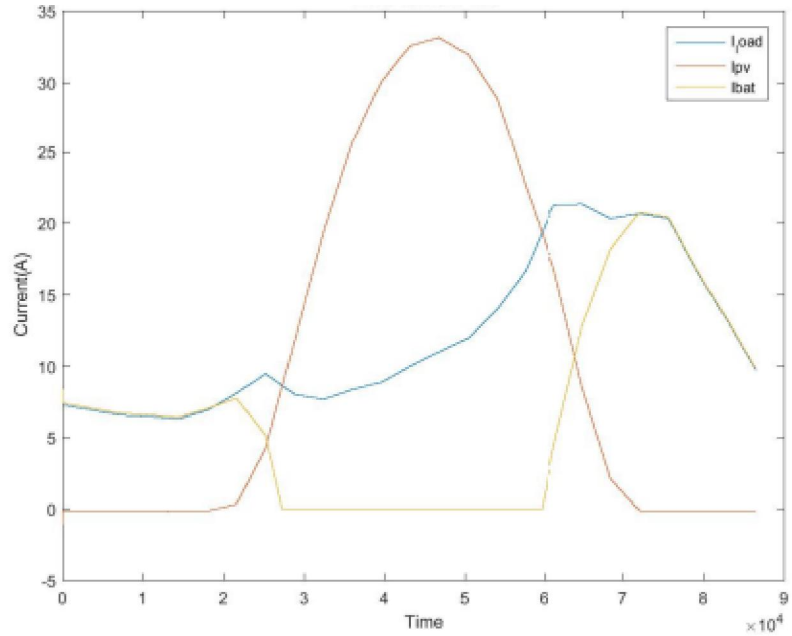

Figure 46 May9

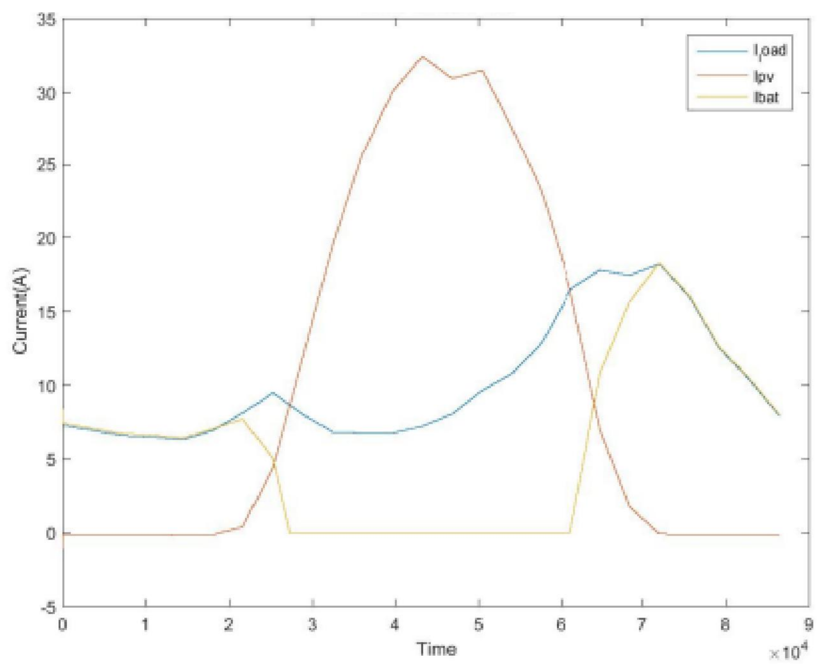

Figure 47 May10

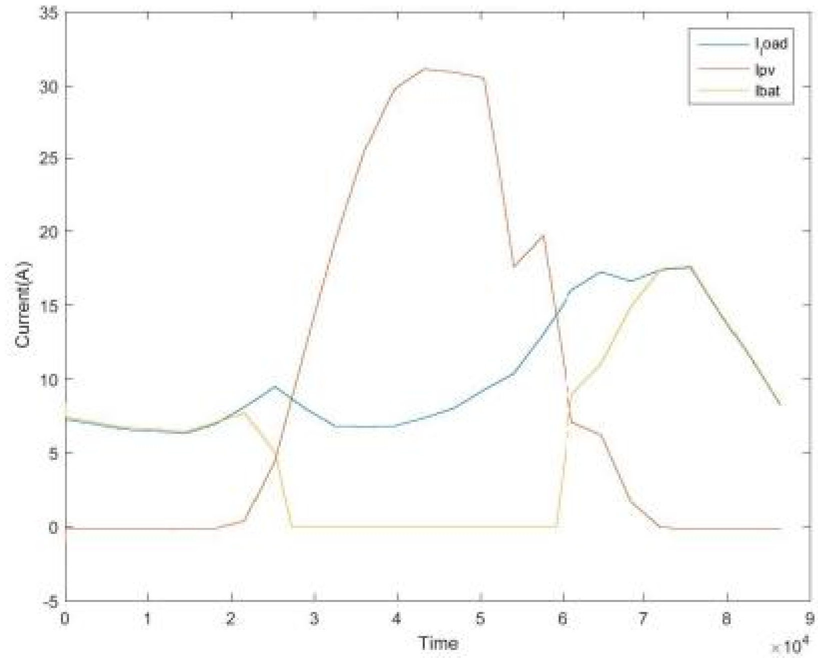

Figure 48 May11

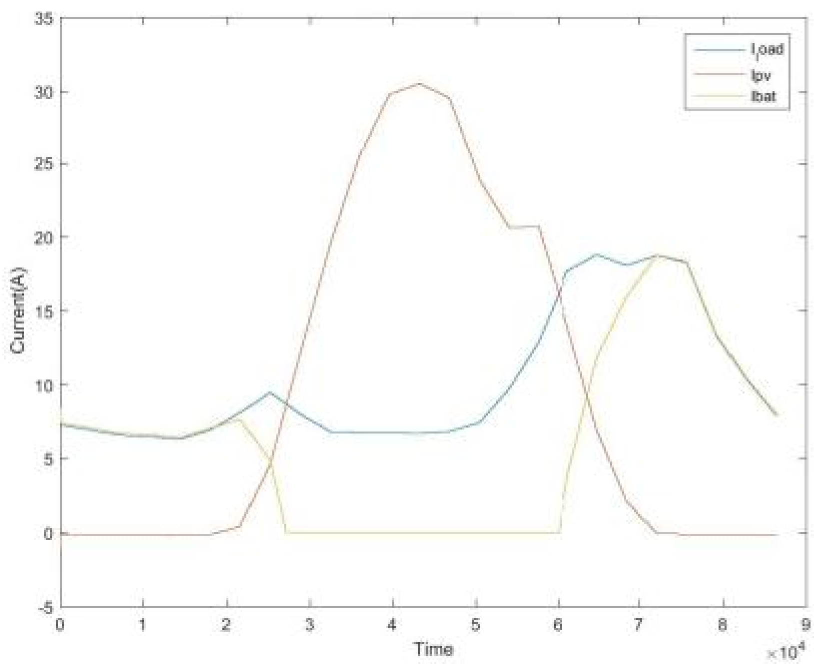

Figure 49 May12

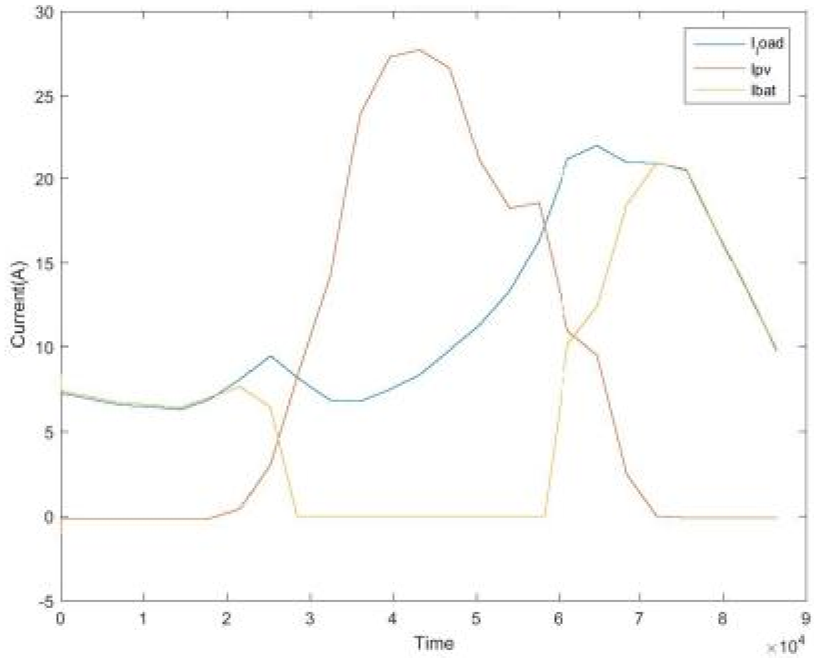

Figure 50 May13

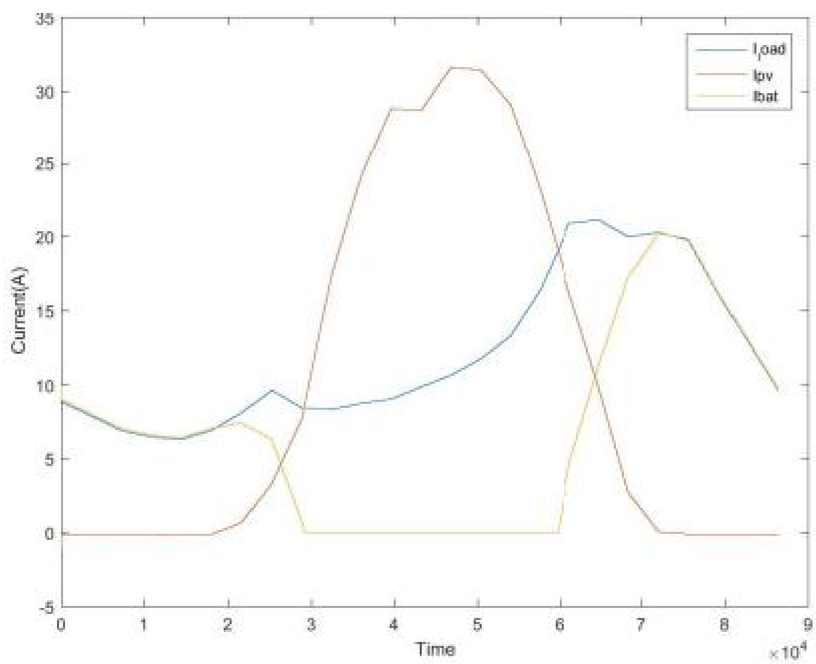

Figure 51 May14

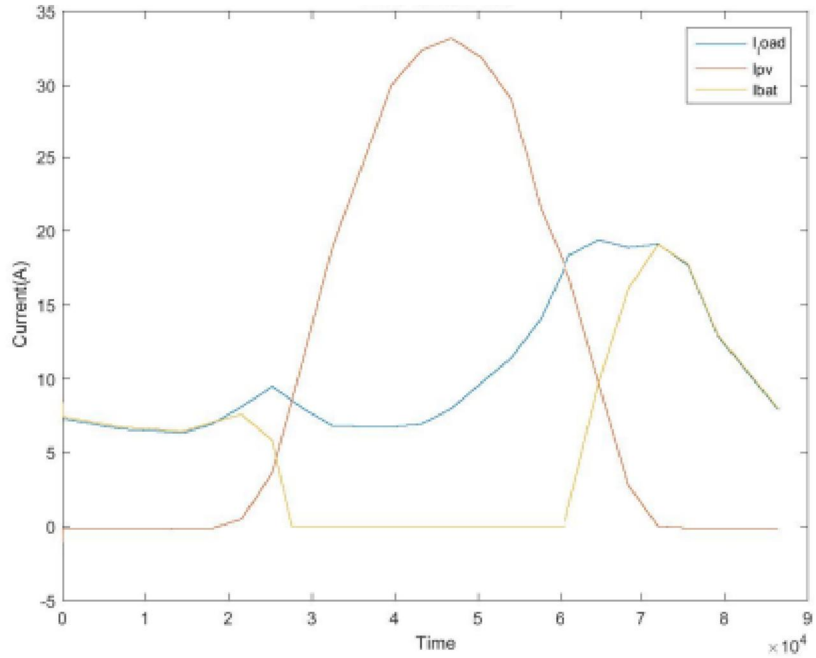

Figure 52 May15

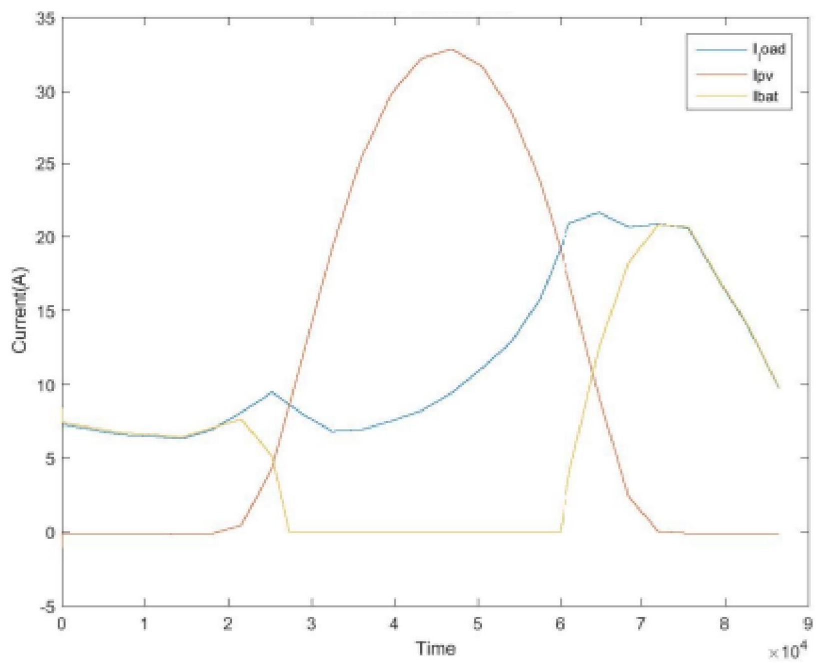

Figure 53 May16

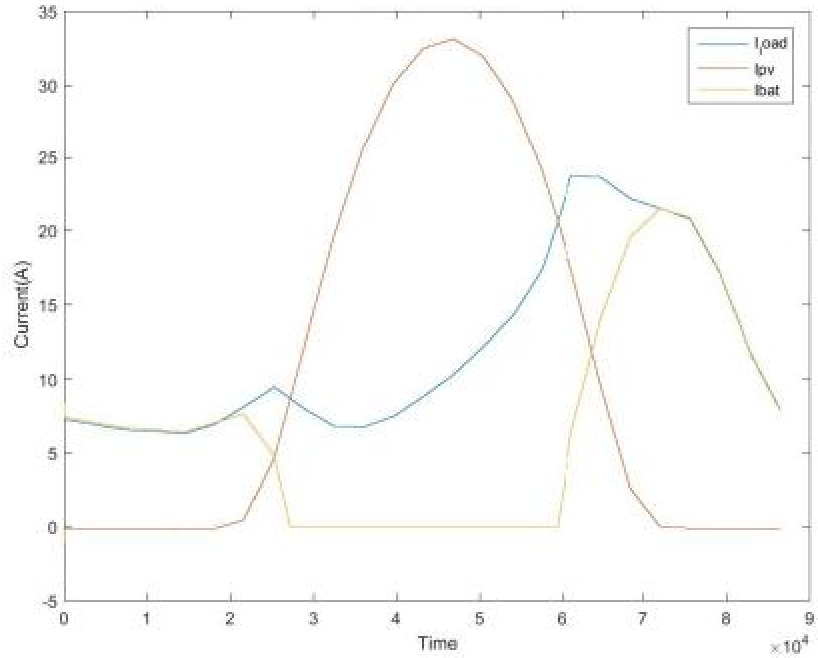

Figure 54 May17

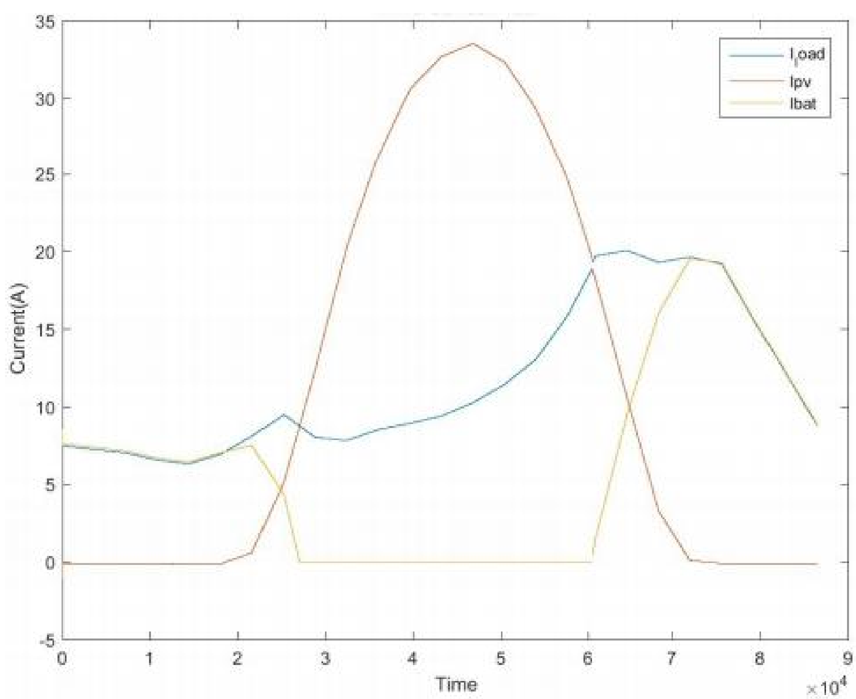

Figure 55 May18

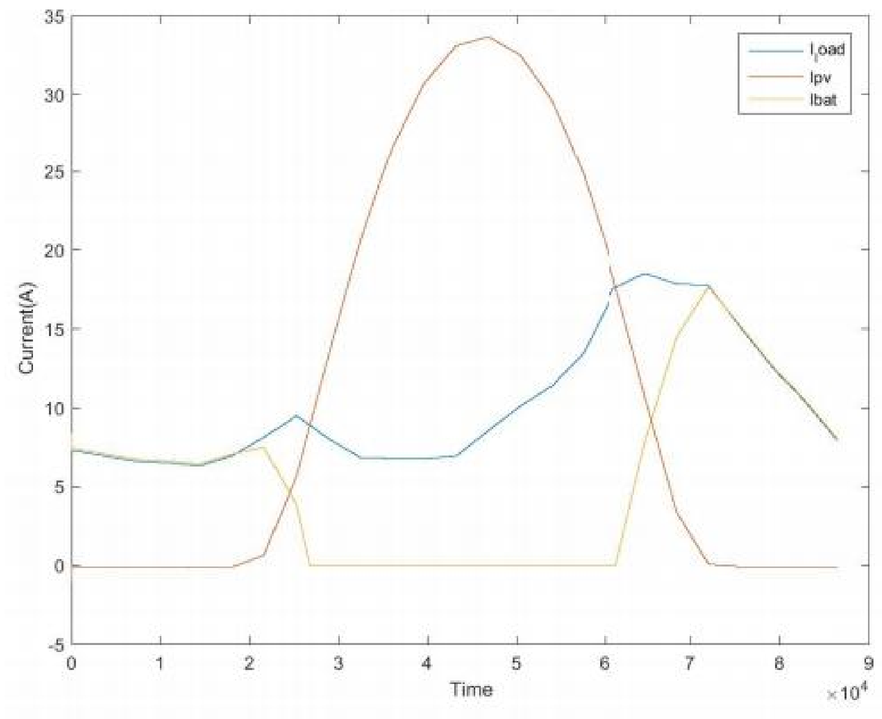

Figure 56 May19

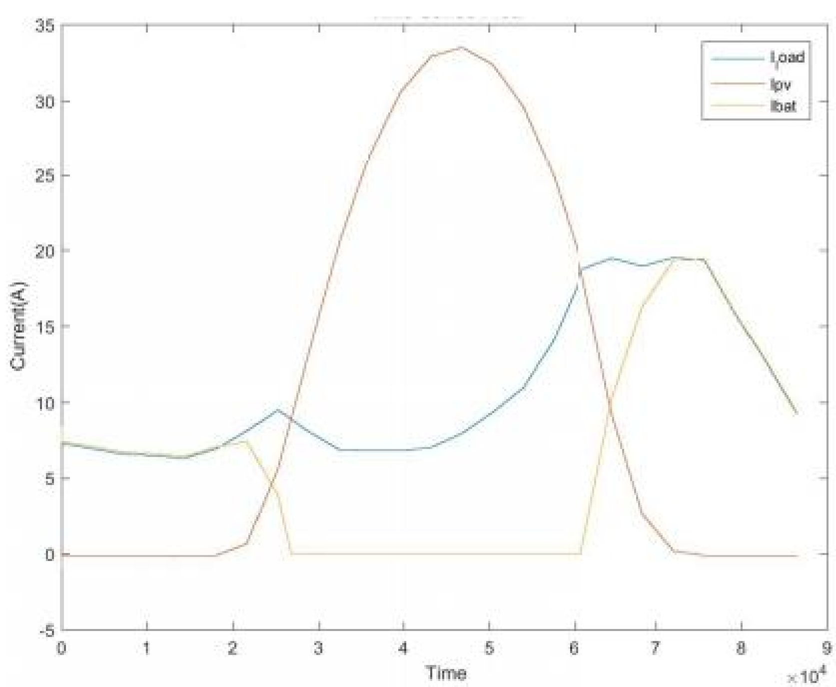

Figure 57 May20

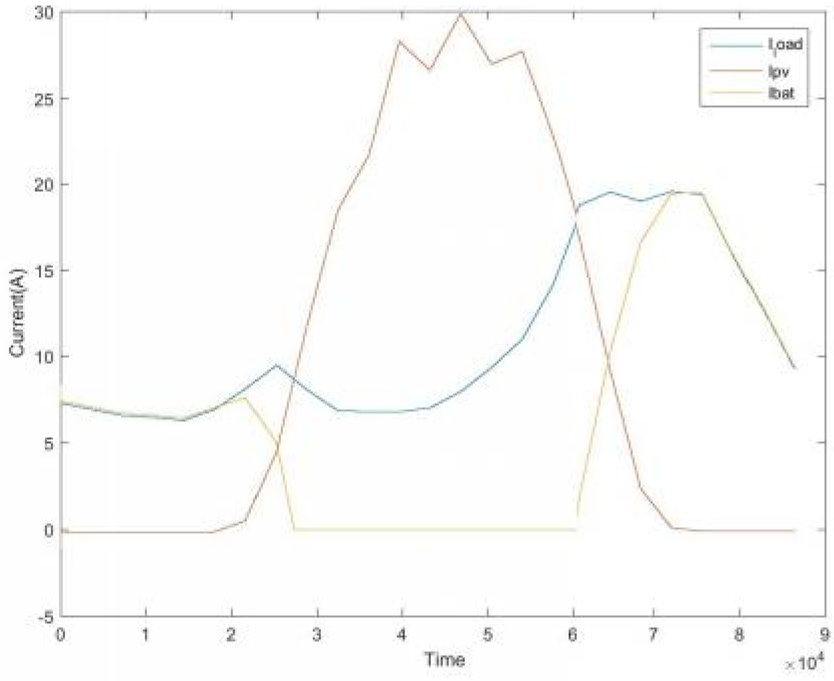

Figure 58 May21

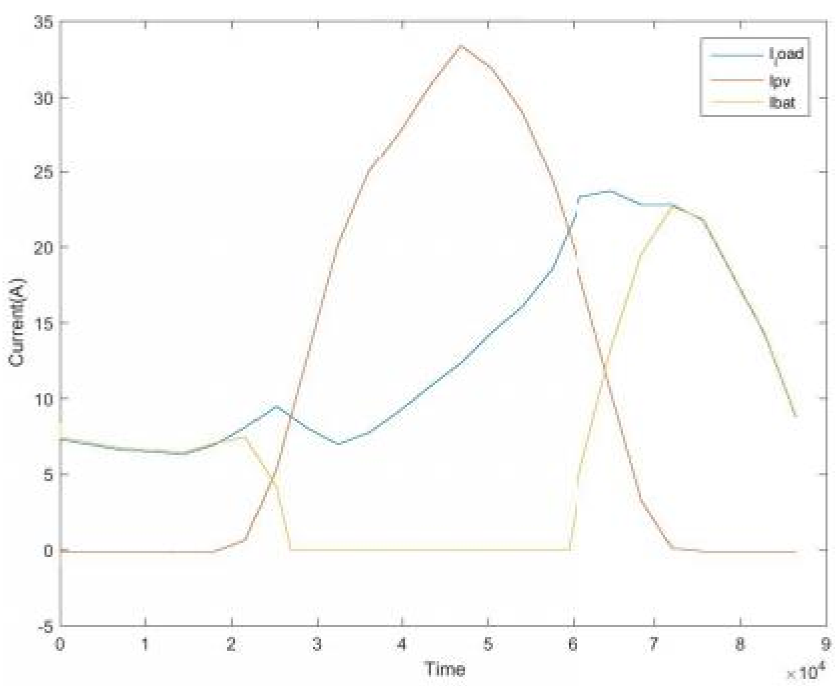

Figure 59 May22

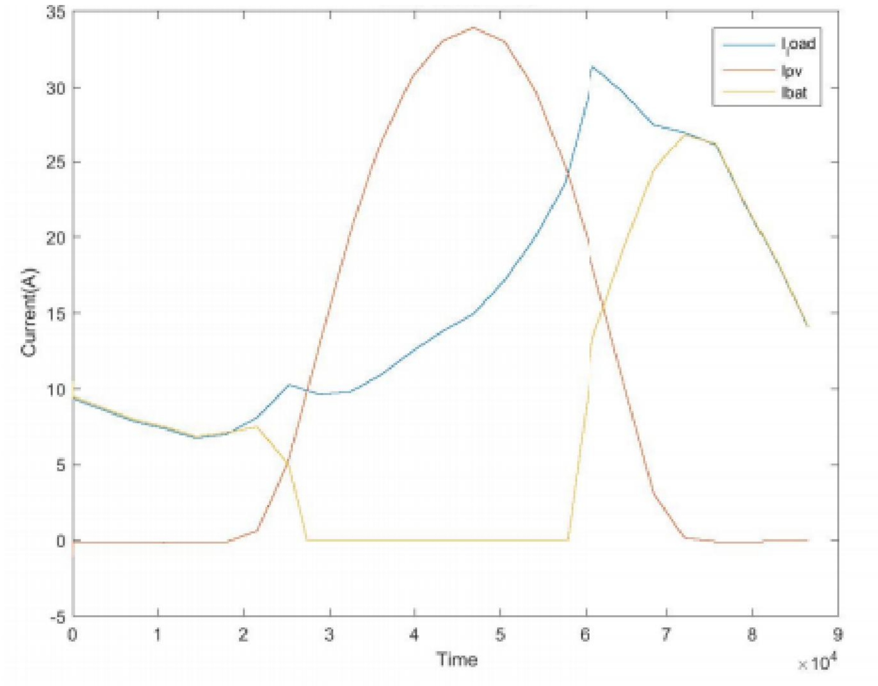

Figure 60 May23

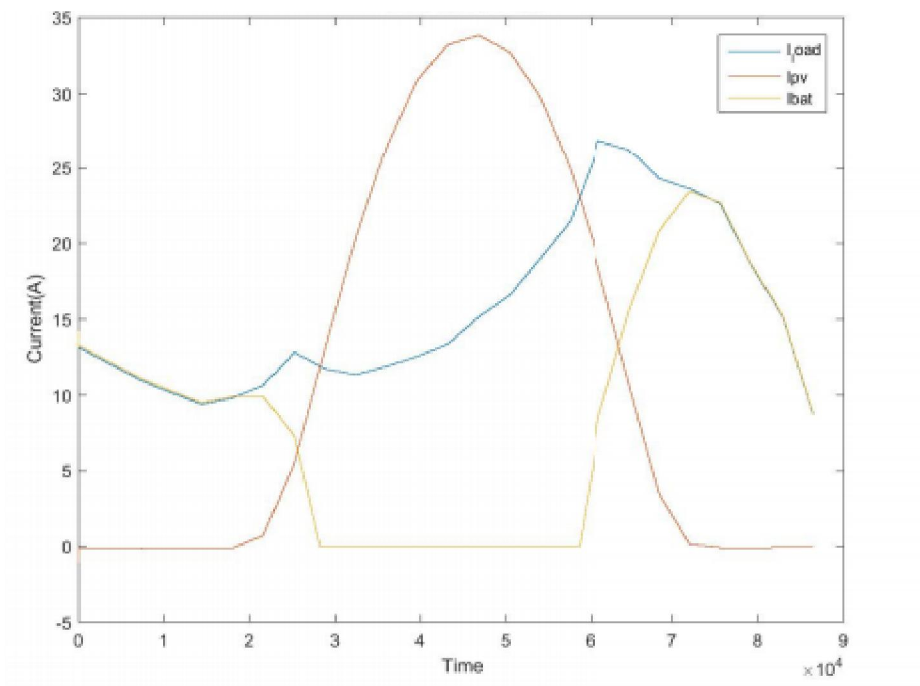

Figure 61 May24

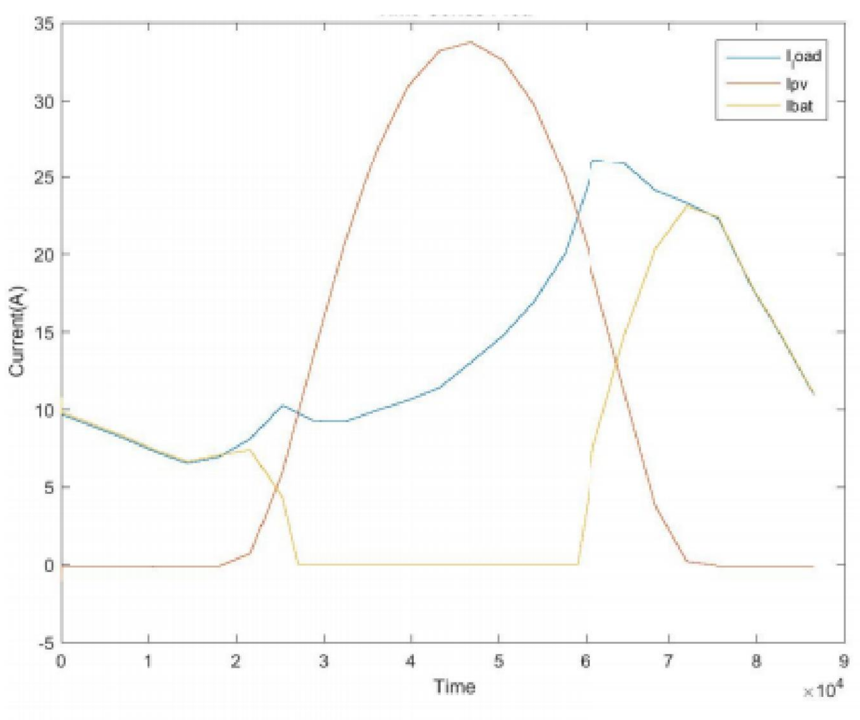

Figure 62 May25

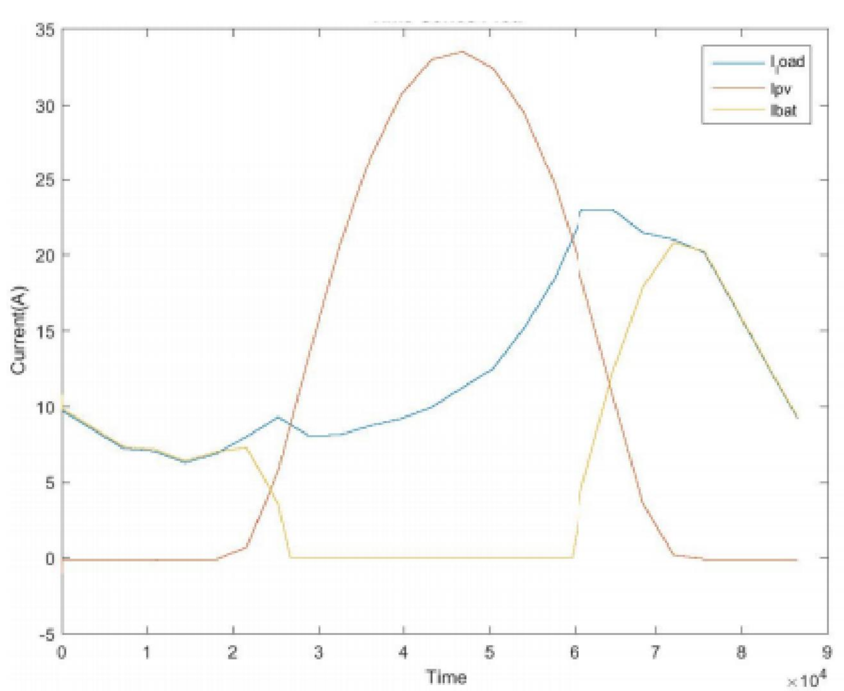

Figure 63 May26

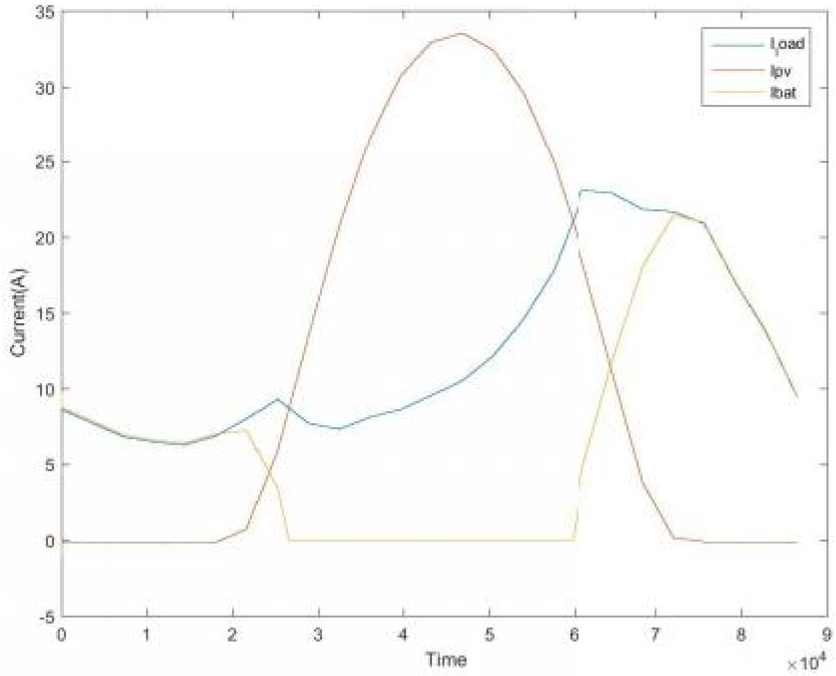

Figure 64 May27

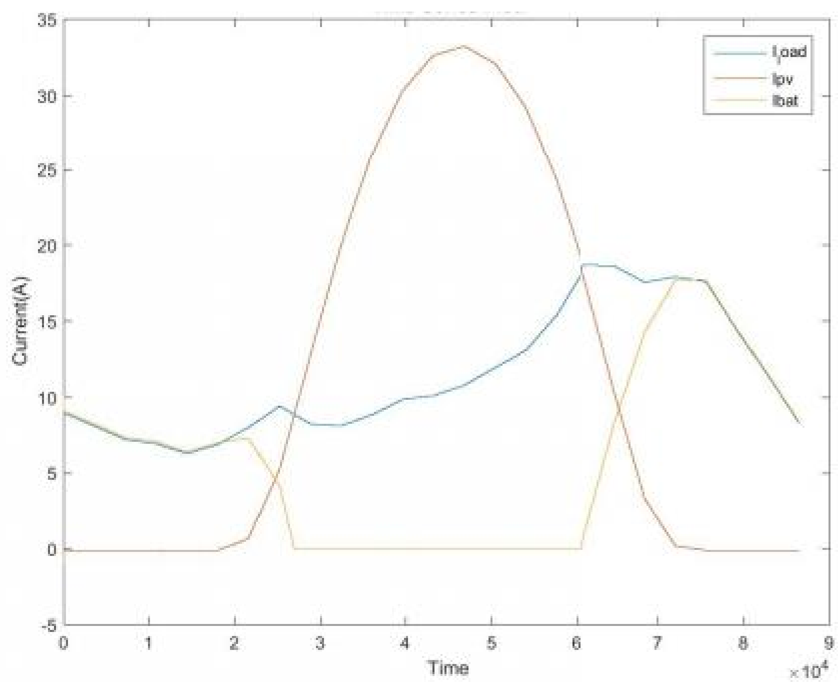

Figure 65 May28

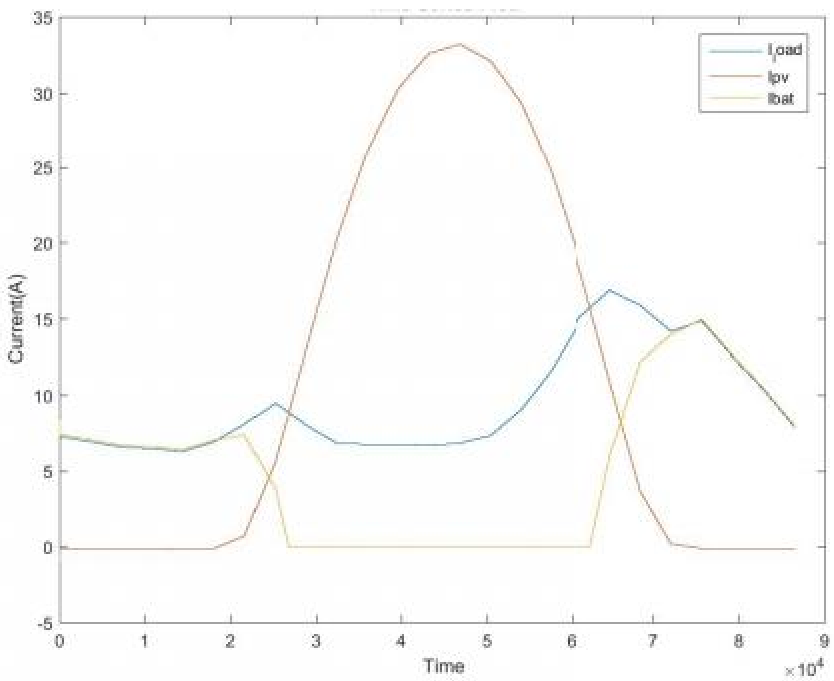

Figure 66 May29

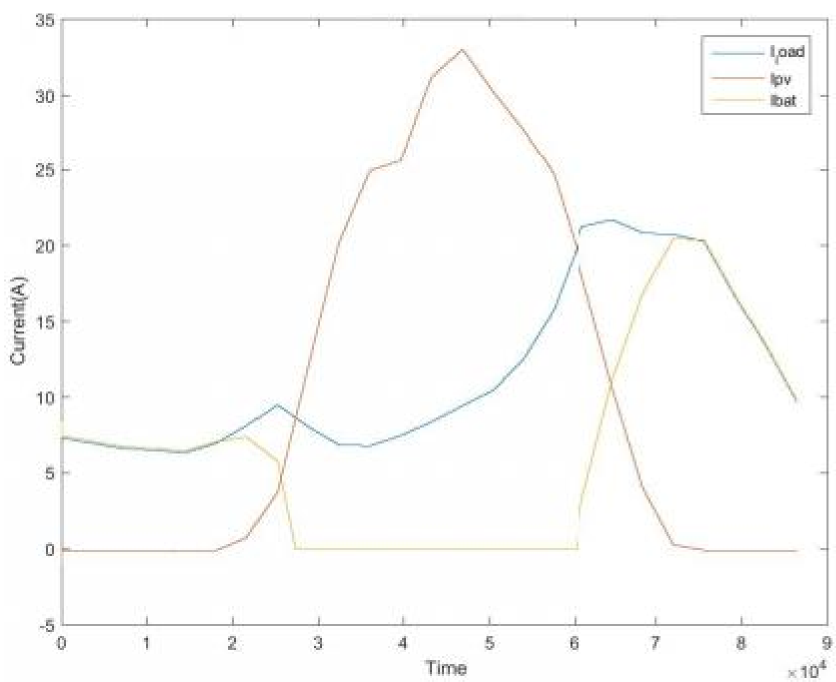

Figure 67 May30

8 References

[1] J. Romm, "Why Used Electric Car Batteries Could Be Crucial To A Clean Energy Future".

[2] E. N. Elkind, "How to Save Money and Clean the Grid with," *REUSE AND REPOWER,* 2014.

[3] J. V. S. S. H. H. J. Hoppmann, "The economic viability of battery storage for residential solar photovoltaic systems-A review and a simulation model," *Renewable and Sustainable Energy Reviews,* 2014.

[4] "https://www.gamry.com/application-notes/EIS/testing-electrochemical-capacitors-part-3-electrochemical-impedance-spectroscopy/," [Online].

[5] "Oregon Green Energy Guide," [Online].

[6] G. Alber, "Electrical Construction and Maintenance," 1 2 2001. [Online].

[7] "https://en.wikipedia.org/wiki/Nickel%E2%80%93metal_hydride_battery," [Online].

[8] "Basics of Electrochemical Impedance Spectroscopy," [Online].

[9] T. Warwick, "Battery Testing with EIS (Electrochemical Impedance Spectroscopy)," 2015.

[10] "Solar PV system Sizing: Step by step approach to design a roof top system and software analysis," [Online].

[11] "https://en.wikipedia.org/wiki/Theory_of_solar_cells," [Online].

[12] S. Kann, "Solar Market Insight Report 2016 Q3," *SEIA,* 2016.

[13] H. W. T. Starrs, "get your power from the sun," *Consumer's Guide,* 2003.

[14] E. A. G. Onokerhoraye, "TRANSITIONING TO SUSTAINABLE," *Centre for Population and Environmental Development (CPED), Benin City, Nigeria,* 2014.

[15] V. C. N. Rajasekaram, "Solar PV in multi-family houses with battery storage," 2015.

[16] A. B. Das, "A Guide to Solar Power Generation in the United Arab Emirates," *MESIA,* 2014.

[17] R. S. R. P. H. K. Akikur, "Comparative study of stand-alone and hybrid solar energy systems suitable for off-grid rural electrification," *Renewable and Sustainable Energy Reviews,* pp. 738-752, 2013.

[18] A. M. A. Ghafoor, "Design and economics analysis of an off-grid PV system for household electrification," *Renewable and Sustainable Energy Reviews,* pp. 496-502, 2015.

[19] M. Shehata, "LATENT HEAT STORAGE FOR AN OFF-GRID PV COOLING SYSTEM IN EGYPT," 2014.

[20] A. G. K. Z. L. G. M. Jafari, "Simulation and analysis of the effect of real-world driving styles in an EV battery performance and aging," *IEEE Transactions on Transportation Electrification,* vol. 1, pp. 391-402, 2015.